Estimation of Net Ecosystem Carbon Exchange for the Conterminous United States by Combining MODIS and AmeriFlux Data

Jingfeng Xiao[1]*, Qianlai Zhuang[2], Dennis D. Baldocchi[3], Beverly E. Law[4], Andrew D. Richardson[5], Jiquan Chen[6], Ram Oren[7], Gregory Starr[8], Asko Noormets[9], Siyan Ma[10], Shashi B. Verma[11], Sonia Wharton[12], Steven C. Wofsy[13], Paul V. Bolstad[14], Sean P. Burns[15], David R. Cook[16], Peter S. Curtis[17], Bert G. Drake[18], Matthias Falk[12], Marc L. Fischer[19], David R. Foster[20], Lianhong Gu[21], Julian L. Hadley[22], David Y. Hollinger[23], Gabriel G. Katul[7] , Marcy Litvak[24], Timothy A. Martin[25], Roser Matamala[26], Steve McNulty[27], Tilden P. Meyers[28], Russell K. Monson[15], J. William Munger[29], Walter C. Oechel[30], Kyaw Tha Paw U[12], Hans Peter Schmid[31], Russell L. Scott[32], Ge Sun[27], Andrew E. Suyker[11], Margaret S. Torn[33]

[1]Department of Earth & Atmospheric Sciences, Purdue Climate Change Research Center, Purdue University, West Lafayette, IN 47907, USA
[2]Department of Earth & Atmospheric Sciences, Department of Agronomy, Purdue Climate Change Research Center, Purdue University, West Lafayette, IN 47907, USA
[3]Atmospheric Science Center, University of California, Berkeley, Berkeley, CA 94720, USA
[4]College of Forestry, Oregon State University, Corvallis, OR 97331, USA
[5]Complex Systems Research Center Institute for the Study of Earth, Oceans and Space, University of New Hampshire, Durham, NH 03824, USA
[6]Department of Environmental Sciences, University of Toledo, Toledo, OH 43606, USA
[7]Nicholas School of the Environment, Duke University, Durham, NC 27708, USA
[8]Department of Biological Sciences, University of Alabama, Tuscaloosa, AL 35487, USA
[9]Department of Forestry and Environmental Resources and Southern Global Change Program, North Carolina State University, Raleigh, NC 27695, USA
[10]Department of Environmental Science, Policy, & Management, University of California, Berkeley, CA 94720, USA
[11]School of Natural Resources, University of Nebraska-Lincoln, Lincoln, NE 68583, USA
[12]Department of Land, Air and Water Resources, University of California, Davis, Davis, CA 95616, USA
[13]Division of Engineering and Applied Science/Department of Earth and Planetary Science, Harvard University, Cambridge, MA 02138, USA
[14]Department of Forest Resources, University of Minnesota, St. Paul, MN 55108, USA
[15]Department of Ecology and Evolutionary Biology, University of Colorado, Boulder, CO 35 80309, USA
[16]Argonne National Laboratory, Environmental Science Division, Argonne, IL 60439, USA
[17]Department of Evolution, Ecology, and Organismal Biology, Ohio State University, Columbus, OH 43210, USA
[18]Smithsonian Environmental Research Center, Edgewater, MD 21037, USA
[19]Lawrence Berkeley National Laboratory, Environmental Energy Technologies Division, Atmospheric Science Department, Berkeley, CA 94720, USA
[20]Harvard Forest and Department of Organismic and Evolutionary Biology, Harvard University, Petersham, MA 01366, USA
[21]Oak Ridge National Laboratory Environmental Sciences Division, Oak Ridge, TN 37831, USA
[22]Harvard Forest, Harvard University, Petersham, MA 01366, USA
[23]USDA Forest Service, Northeastern Research Station, Durham, NH 03824, US47 A

[24]Department of Biology, University of New Mexico, Albuquerque, NM 87131, USA
[25]University of Florida, Gainesville, FL 32611, USA
[26]Argonne National Laboratory, Biosciences Division, Argonne, IL 60439, USA
[27]USDA-Forest Service, Southern Research Station, Raleigh, NC 27606, USA
[28]NOAA/ARL, Atmospheric Turbulence and Diffusion Division, Oak Ridge, TN 37831, USA
[29]Department of Earth and Planetary Sciences, Harvard University, Cambridge, MA 02138, USA
[30]Department of Biology, San Diego State University, San Diego, CA 92182, USA
[31]Department of Geography, Indiana University, Bloomington, IN 47405, USA
[32]USDA-ARS Southwest Watershed Research Center, Tucson, AZ 85719, USA
[33]Lawrence Berkeley National Laboratory, Earth Science Division, Berkeley, CA 94720, USA

03/22/2008

This work was supported by the Director, Office of Science, Office of Basic Energy Sciences, of the U.S. Department of Energy under Contract No. DE-AC02-05CH11231.

Estimation of Net Ecosystem Carbon Exchange for the Conterminous United States by Combining MODIS and AmeriFlux Data

Jingfeng Xiao[1*], Qianlai Zhuang[2], Dennis D. Baldocchi[3], Beverly E. Law[4], Andrew D. Richardson[5], Jiquan Chen[6], Ram Oren[7], Gregory Starr[8], Asko Noormets[9], Siyan Ma[10], Shashi B. Verma[11], Sonia Wharton[12], Steven C. Wofsy[13], Paul V. Bolstad[14], Sean P. Burns[15], David R. Cook[16], Peter S. Curtis[17], Bert G. Drake[18], Matthias Falk[12], Marc L. Fischer[19], David R. Foster[20], Lianhong Gu[21], Julian L. Hadley[22], David Y. Hollinger[23], Gabriel G. Katul[7], Marcy Litvak[24], Timothy A. Martin[25], Roser Matamala[26], Steve McNulty[27], Tilden P. Meyers[28], Russell K. Monson[15], J. William Munger[29], Walter C. Oechel[30], Kyaw Tha Paw U[12], Hans Peter Schmid[31], Russell L. Scott[32], Ge Sun[27], Andrew E. Suyker[11], Margaret S. Torn[33]

[1]Department of Earth & Atmospheric Sciences, Purdue Climate Change Research Center, Purdue University, West Lafayette, IN 47907, USA

[2]Department of Earth & Atmospheric Sciences, Department of Agronomy, Purdue Climate Change Research Center, Purdue University, West Lafayette, IN 47907, USA

[3]Atmospheric Science Center, University of California, Berkeley, Berkeley, CA 94720, USA

[4]College of Forestry, Oregon State University, Corvallis, OR 97331, USA

[5]Complex Systems Research Center Institute for the Study of Earth, Oceans and Space, University of New Hampshire, Durham, NH 03824, USA

[6]Department of Environmental Sciences, University of Toledo, Toledo, OH 43606, USA

[7]Nicholas School of the Environment, Duke University, Durham, NC 27708, USA

[8]Department of Biological Sciences, University of Alabama, Tuscaloosa, AL 35487, USA

[9]Department of Forestry and Environmental Resources and Southern Global Change Program, North Carolina State University, Raleigh, NC 27695, USA

[10]Department of Environmental Science, Policy, & Management, University of California, Berkeley, CA 94720, USA

[11]School of Natural Resources, University of Nebraska-Lincoln, Lincoln, NE 68583, USA

[12]Department of Land, Air and Water Resources, University of California, Davis, Davis, CA 95616, USA

[13]Division of Engineering and Applied Science/Department of Earth and Planetary Science, Harvard University, Cambridge, MA 02138, USA

[14]Department of Forest Resources, University of Minnesota, St. Paul, MN 55108, USA

[15]Department of Ecology and Evolutionary Biology, University of Colorado, Boulder, CO 80309, USA

[16]Argonne National Laboratory, Environmental Science Division, Argonne, IL 60439, USA

[17]Department of Evolution, Ecology, and Organismal Biology, Ohio State University, Columbus, OH 43210, USA

[18]Smithsonian Environmental Research Center, Edgewater, MD 21037, USA

[19]Lawrence Berkeley National Laboratory, Environmental Energy Technologies Division, Atmospheric Science Department, Berkeley, CA 94720, USA

[20]Harvard Forest and Department of Organismic and Evolutionary Biology, Harvard University, Petersham, MA 01366, USA

[21]Oak Ridge National Laboratory Environmental Sciences Division, Oak Ridge, TN 37831, USA

[22]Harvard Forest, Harvard University, Petersham, MA 01366, USA

[23]USDA Forest Service, Northeastern Research Station, Durham, NH 03824, USA

[24]Department of Biology, University of New Mexico, Albuquerque, NM 87131, USA

[25]University of Florida, Gainesville, FL 32611, USA

[26]Argonne National Laboratory, Biosciences Division, Argonne, IL 60439, USA

[27]USDA-Forest Service, Southern Research Station, Raleigh, NC 27606, USA

[28]NOAA/ARL, Atmospheric Turbulence and Diffusion Division, Oak Ridge, TN 37831, USA

[29]Department of Earth and Planetary Sciences, Harvard University, Cambridge, MA 02138, USA

[30]Department of Biology, San Diego State University, San Diego, CA 92182, USA

[31]Department of Geography, Indiana University, Bloomington, IN 47405, USA

[32]USDA-ARS Southwest Watershed Research Center, Tucson, AZ 85719, USA

[33]Lawrence Berkeley National Laboratory, Earth Science Division, Berkeley, CA 94720, USA

*Corresponding author: jing@purdue.edu (Tel: 765-496-8678; Fax: 496-1210)

Agricultural and Forest Meteorology

Submitted: 03/22/2008

Abstract

Eddy covariance flux towers provide continuous measurements of net ecosystem carbon exchange (NEE) for a wide range of climate and biome types. However, these measurements only represent the carbon fluxes at the scale of the tower footprint. To quantify the net exchange of carbon dioxide between the terrestrial biosphere and the atmosphere for regions or continents, flux tower measurements need to be extrapolated to these large areas. Here we used remotely-sensed data from the Moderate Resolution Imaging Spectrometer (MODIS) instrument on board NASA's Terra satellite to scale up AmeriFlux NEE measurements to the continental scale. We first combined MODIS and AmeriFlux data for representative U.S. ecosystems to develop a predictive NEE model using a regression tree approach. The predictive model was trained and validated using NEE data over the periods 2000-2004 and 2005-2006, respectively. We found that the model predicted NEE reasonably well at the site level. We then applied the model to the continental scale and estimated NEE for each 1 km × 1 km cell across the conterminous U.S. for each 8-day period in 2005 using spatially-explicit MODIS data. The model generally captured the expected spatial and seasonal patterns of NEE. Our study demonstrated that our empirical approach is effective for scaling up eddy flux NEE measurements to the continental scale and producing wall-to-wall NEE estimates across multiple biomes. Our estimates may provide an independent dataset from simulations with biogeochemical models and inverse modeling approaches for examining the spatiotemporal patterns of NEE and constraining terrestrial carbon budgets for large areas.

Keywords: Net ecosystem carbon exchange; MODIS; AmeriFlux; NEE; Regression tree; Eddy covariance

1. Introduction

Net ecosystem carbon exchange (NEE), the difference of photosynthetic uptake and release of carbon dioxide (CO_2) by respiration from autotrophs (plants) and heterotrophs (e.g., microbial decomposition), represents the net exchange of carbon dioxide (CO_2) between terrestrial ecosystems and the atmosphere (Law et al., 2006). The quantification of NEE for regions, continents, or the globe can improve our understanding of the feedbacks between the terrestrial biosphere and the atmosphere in the context of global change and facilitate climate policy-making. The estimation of NEE over large areas is therefore of scientific and political importance.

To date, numerous techniques have been used to estimate NEE (Chen et al., 2004). Atmospheric inverse models (e.g., Tans et al., 1990; Denning et al., 1996; Fan et al., 1998; Gurney et al., 2002; Deng et al., 2007) and biogeochemical models (Parton et al., 1993; Potter et al., 1993; Running and Hunt, 1993; Field et al., 1995; Zhuang et al., 2003; Xiao et al., 2008) have been used to provide aggregated information on carbon balances over large areas during the past two decades. The accuracy of the estimates by atmospheric inverse models is limited by the sparseness of the CO_2 observation network and their biased placement in the marine boundary layers (Tans et al., 1990; Denning et al., 1996; Fan et al., 1998). Moreover, this approach does not provide information about which ecosystems are contributing to the sinks/sources or the processes involved (Janssens et al., 2003). Most biogeochemical models, however, are dependent on site-level parameterizations, which limits the accuracy of model simulations over large areas. Moreover, besides atmospheric CO_2 and climate variability, factors such as land use/land cover change (McGuire et al., 2001), disturbances (Zhuang et al., 2002; Law et al., 2004), N deposition (Nadelhoffer et al., 1999), and management practices

(Xiao and Moody, 2004a; Magnani et al., 2007) significantly affect NEE. It is still a challenge for most biogeochemical models to consider all these factors due to model limitations and/or lack of input data.

At the site level, eddy covariance flux towers have been providing continuous measurements of ecosystem-level exchanges of carbon at half-hourly or hourly time steps since the early 1990s (Wofsy et al., 1993; Baldocchi et al., 2001). At present, over 400 eddy covariance flux towers are operating on a long-term and continuous basis over the globe (FLUXNET, 2008). This global network encompasses a large range of climate and biome types (Baldocchi et al., 2001), and provides the most extensive, reliable, and longest measurements of NEE. However, these measurements only represent the fluxes at the scale of the tower footprint (Running et al., 1999), up to several square kilometers (Schmid, 1994). To quantify the net exchange of CO_2 between the terrestrial biosphere and the atmosphere, we need to scale up these flux tower measurements to regions, continents, or the globe.

Satellite remote sensing is a potentially valuable tool for scaling up NEE to large areas (Running et al., 1999). There have been several studies developing methods for integration of flux data with remote sensing data to quantify NEE over large areas. For example, Yamaji et al. (2007) linked MODIS (Moderate Resolution Imaging Spectroradiometer) data to flux tower NEE data for regional extrapolation to deciduous broadleaf forests over Japan. Wylie et al. (2007) estimated NEE for grasslands in the northern Great Plains using satellite data and flux tower NEE measurements. Papale and Valentini (2003) estimated NEE for European forests using flux tower data and NOAA AVHRR satellite data. Mahadevan et al. (2008) used eddy covariance flux data to calibrate the vegetation photosynthesis and respiration model (VPRM) for estimating NEE from MODIS data at an hourly time step. Similar to process-based

biogeochemical models, this empirical model is also based on site-level parameterizations. Despite these efforts, to our knowledge, no study has scaled up flux tower NEE measurements to the continental scale and produced spatially-explicit estimates of NEE across multiple biomes.

Here we combined MODIS and eddy covariance flux data to scale up flux tower NEE measurements to the continental scale and produce wall-to-wall NEE estimates for the conterminous U.S. First, we developed a predictive NEE model based on site-specific MODIS and AmeriFlux data. Second, we validated the performance of the model with AmeriFlux data. Third, we applied the model to estimate NEE for each 1 km × 1 km cell across the conterminous U.S. for each 8-day period in 2005 using wall-to-wall MODIS data. Finally, we examined the spatiotemporal patterns of NEE.

2. Methods

2.1. Regression tree

A regression tree approach was used to scale up tower-based NEE to the continental scale. Regression tree algorithms predict class membership by recursively partitioning a dataset into more homogeneous subsets. The partitioning process splits each parent node into two child nodes, and each child node is treated as a potential parent node (Breiman et al., 1984). These algorithms produce rule-based models containing one or more rules, each of which is a set of conditions associated with a linear submodel. Regression tree models can therefore account for a nonlinear relationship between predictive and target variables (Yang et al., 2003). These models also allow both continuous and discrete variables as input variables (Yang et al., 2003). In addition, regression tree approaches are proven not only more effective than simple techniques including multivariate linear regression, but also easier to understand than neural

networks (Huang and Townshend, 2003). Piecewise regression models were selected as the most appropriate approach for scaling the flux tower data to ecoregions (Wylie et al., 2007).

We used the regression tree algorithm implemented in the commercial software called Cubist. Cubist has been used to estimate percent land cover (Huang and Townshend, 2003), impervious area (Yang et al., 2003), forest biomass (Salajanu et al., 2005), and ecosystem carbon fluxes (Wylie et al., 2007). We chose Cubist to construct a predictive NEE model based on AmeriFlux NEE and satellite data. Cubist is a powerful tool for generating rule-based predictive models. The predictive accuracy of a rule-based model can be improved by combining it with an instance-based/nearest-neighbor model that predicts the target value of a new case using the average predicted values of the *n* most similar cases. The use of the composite model can improve the predictive accuracy relative to the rule-based model alone. Cubist can also generate committee models made up of several rule-based models, and each member of the committee model predicts the target value for a case and the member's predictions are averaged to give a final prediction.

Cubist uses three statistical measures to measure the quality of the constructed regression tree model, including average error, relative error, and product-moment correlation coefficient. The average error is calculated as (Yang et al., 2003):

$$AE = \frac{1}{N}\sum_{i=1}^{N}\left|y_i - \hat{y}_i\right| \quad (1)$$

where AE is the average error of a tree model, N is the number of samples used to establish the tree, and y_i and $\hat{y}_i$ are the actual and predicted values of the response variable, respectively. The relative error is calculated as (Yang et al., 2003):

$$RE = \frac{AE(T)}{AE(\mu)} \quad (2)$$

where RE is the relative error of a tree model, AE(T) is the average error of the tree model, and AE(μ) is the average error that would result from always predicting the mean value. All the three statistical measures provided by Cubist were used to evaluate the performance of the tree model.

2.2. Explanatory variables

NEE is the difference between two large carbon fluxes of photosynthesis and respiration (Law et al., 1999). It is influenced by a variety of physical, physiological, atmospheric, hydrologic, and edaphic variables. At the leaf level, photosynthesis or gross primary productivity (GPP) is influenced by several factors, including incoming solar radiation, air temperature, vapor pressure deficit, soil moisture, and nitrogen availability (Clark et al., 1999, 2004). At the ecosystem level, GPP is also influenced by leaf area index (LAI) and canopy phenology. Ecosystem respiration (R_e) includes autotrophic (R_a) and heterotrophic respiration (R_h). Soil respiration is the largest component of ecosystem respiration. Because autotrophic and heterotrophic activity belowground is controlled by rooting systems and substrate availability, soil respiration is strongly linked to plant metabolism, photosynthesis and litterfall (Ryan and Law, 2005). R_a can be empirically modeled as a function of air temperature and tissue carbon (foliage, stem, roots), whereas R_h is often modeled as a function of substrate availability, soil temperature and soil moisture (Ryan and Law, 2005). At the stand or regional level, NEE is significantly affected by disturbances from fire and harvest (Law et al., 2004) and fractional vegetation cover (DeFries et al., 2002).

Many of these factors influencing NEE can be assessed by satellite remote sensing. Optical remote sensing systems measure the surface reflectance, the fraction of solar energy that is reflected by the Earth's surface. For a given wavelength, different vegetation types

and/or plant species may have different reflectance (Schmidt and Skidmore, 2003). The reflectance of the same vegetation type also depends on wavelength region, biophysical properties (e.g., biomass, leaf area, and stand age), soil moisture, and sun-object-sensor geometry (Ranson et al., 1985; Penuelas et al., 1993). Therefore, reflectance values from multiple spectral bands can provide useful information for estimating NEE. Moreover, surface reflectance can be used to develop vegetation indices and biophysical parameters that can account for factors influencing NEE, such as the enhanced vegetation index (EVI), the land surface temperature (LST), the normalized difference water index (NDWI), the fraction of photosynthetically active radiation absorbed by vegetation canopies (fPAR), and LAI.

The normalized difference vegetation index (NDVI) captures the contrast between the visible-red and near-infrared reflectance of vegetation canopies. It is defined as:

$$NDVI = \frac{\rho_{nir} - \rho_{red}}{\rho_{nir} + \rho_{red}} \quad (3)$$

where ρ_{red} and ρ_{nir} are the visible-red and near-infrared reflectance, respectively. NDVI is closely correlated to the fraction of photosynthetically active radiation (fPAR) absorbed by vegetation canopies (Asrar et al., 1984; Law and Waring, 1994) and photosynthetic activity (Xiao and Moody, 2004b). NDVI is also related to vegetation biomass (Myneni et al., 2001) and fractional vegetation cover (Xiao and Moody, 2005). However, NDVI has several limitations, including saturation in a multilayer closed canopy and sensitivity to both atmospheric aerosols and soil background (Huete et al., 2002; Xiao and Moody, 2005). To account for these limitations of NDVI, Huete et al. (1997) developed the improved vegetation index, EVI:

$$EVI = 2.5 \times \frac{\rho_{nir} - \rho_{red}}{\rho_{nir} + (6 \times \rho_{red} - 7.5 \times \rho_{blue}) + 1} \quad (4)$$

where ρ_{nir}, ρ_{red}, and ρ_{blue} are the spectral reflectance at the near-infrared, red, and blue wavelengths, respectively.

The LST derived from MODIS is a measure of the soil temperature at the surface. The MODIS LST agreed with in situ measured LST within 1 K in the range 263-322 K (Wan et al., 2002). LST is likely a good indicator of R_e as both R_a and R_H are significantly affected by air/surface temperature. Rahman et al. (2005) demonstrated that satellite-derived LST was strongly correlated with R_e.

As the shortwave infrared (SWIR) spectral band is sensitive to vegetation water content and soil moisture, a combination of NIR and SWIR bands have been used to derive water-sensitive vegetation indices (Ceccato et al., 2002). Gao (1996) developed the NDWI from satellite data to measure vegetation liquid water:

$$NDWI = \frac{\rho_{nir} - \rho_{swir}}{\rho_{nir} + \rho_{swir}} \quad (5)$$

where ρ_{swir} is the reflectance at the shortwave infrared (SWIR) spectral band. The NDWI was shown to be strongly correlated with leaf water content (equivalent water thickness (EWT), g H_2O/m^2) (Jackson et al., 2004) and soil moisture (Fensholt and Sandholt, 2003) over time. It was incorporated into the vegetation photosynthesis model (VPM) as a water scalar for estimating GPP (Xiao et al., 2005). Yet, there is still a question as to whether NDWI provides useful information on canopy water stress status that affects photosynthesis because of its sensitivity to the relatively small changes in relative water content observed in natural vegetation, and inability to discern changes in canopy biomass from changes in canopy moisture status (Hunt and Rock, 1989; Gao 1996).

250 Satellite data can also provide estimates for LAI and fPAR. These two variables
251 characterize vegetation canopy functioning and energy absorption capacity (Myneni et al.,
252 2002), and are key parameters in most ecosystem productivity and biogeochemical models due
253 to their high correlation with GPP (Sellers et al., 1997).
254 We therefore selected surface reflectance, EVI, LST, NDWI, fPAR, and LAI as
255 explanatory variables. All these variables were derived from MODIS data, which also avoided
256 the complications and difficulties to merge disparate data sources.

257 *2.3. Data*

258 We obtained the following three types of data: NEE from eddy covariance flux towers,
259 explanatory variables derived from MODIS data, and a land cover map derived from MODIS.

260 *2.3.1 AmeriFlux data*

261 The AmeriFlux network coordinates regional analysis of observations from eddy
262 covariance flux towers across North America, Central America, and South America (Law,
263 2006). We obtained the Level 4 NEE product for 42 AmeriFlux sites for the period 2000-2006
264 from the AmeriFlux website (http://public.ornl.gov/ameriflux/) (Table 1). These sites are
265 distributed across the conterminous U.S. (Fig. 1), and cover a range of vegetation types
266 including forests, shrublands, savannas, grasslands, and croplands (Table 1). Moreover, the
267 distribution of these sites in the mean annual climate space (Fig. 2) indicates that they cover
268 typical U.S. climate types. In addition, they also include some forest sites at different times
269 since stand replacing disturbance, which are located in disturbance clusters of sites. We
270 therefore believe that these sites are roughly representative of U.S. ecosystem and climate
271 types.

272 [insert Fig. 1 about here]

[insert Fig. 2 about here]

The Level 4 product consists of two types of NEE data, including standardized (NEE_st) and original (NEE_or) NEE (AmeriFlux, 2007). NEE_st was calculated using CO_2 flux estimated by the eddy covariance method, which includes summation with CO_2 storage in the canopy air space that was obtained from the discrete approach (single point on the top of the tower) for all the sites, whereas NEE_or was calculated using the storage obtained from within canopy CO_2 profile measurements in relatively tall forest canopies or from the discrete approach. The average data coverage during a year is only 65% due to system failures or data rejection, and therefore robust and consistent gap filling methods are required to provide complete data sets (Falge et al., 2001). Both NEE_st and NEE_or were filled using the Marginal Distribution Sampling (MDS) method (Reichstein et al., 2005) and the Artificial Neural Network (ANN) method (Papale and Valentini, 2003). The ANN method was generally, if only slightly, superior to the MDS method (Moffat et al., 2007). Therefore, we used the gap-filled NEE data based on the ANN method. For each site, if the percentage of the remaining missing values for NEE_st was lower than that for NEE_or, we selected NEE_or; otherwise, we used NEE_st.

The Level 4 product consists of NEE data with four different time steps, including half-hourly, daily, weekly (8-day), and monthly. We used 8-day NEE data (g C m^{-2} day^{-1}) to match the compositing intervals of MODIS data. Moreover, the average NEE over such a period was shown to largely eliminate micrometeorological sampling errors, with the remaining spatial variability representing variation in ecosystem attributes such as LAI (Oren et al. 2006), here accounted for by data from MODIS.

2.3.2. MODIS data

296 MODIS is a key instrument on board the NASA's Terra and Aqua satellites. The Terra
297 MODIS and Aqua MODIS view the entire Earth's surface every one to two days, acquiring
298 data in 36 spectral bands and with the spatial resolution of 250m, 500m, and 1km. We used the
299 following four MODIS data products, including surface reflectance (MOD09A1; Vermote and
300 Vermeulen, 1999), daytime and nighttime LST (MOD11A2; Wan et al., 2002), EVI
301 (MOD13A1; Huete et al., 2002), and LAI/fPAR (MOD15A2; Myneni et al., 2002). Surface
302 reflectance data consist of reflectance values of seven spectral bands: blue (459-479 nm), green
303 (545-565 nm), red (620-670 nm), near infrared (841-875 nm, 1230-1250 nm), shortwave
304 infrared (1628-1652 nm, 2105-2155 nm). Surface reflectance and EVI are at a spatial
305 resolution of 500m, while LAI, fPAR, and LAI are at spatial resolution of 1km. Surface
306 reflectance, fPAR, and LAI are at a temporal resolution of 8 days, while EVI is at a temporal
307 resolution of 16 days.
308 For each AmeriFlux site, we obtained the MODIS ASCII subsets (Collection 4)
309 consisting of 7 km × 7 km regions centered on the flux tower from the Oak Ridge National
310 Laboratory's Distributed Active Archive Center (ORNL DAAC, 2006). We extracted average
311 values for the central 3 × 3 km area within the 7 × 7 km cutouts to better represent the flux
312 tower footprint (Schmid, 2002; Rahman et al., 2005). For each variable, we determined the
313 quality of the value of each pixel within the area using the quality assurance (QA) flags
314 included in the product. At each time step, we averaged the values of each variable using the
315 pixels with good quality within the area to represent the values at the flux site. If none of the
316 values within the 3 × 3 km area was of good quality, we treated the period as missing. Each 16-
317 day EVI value was split into two 8-day values to correspond with the compositing interval of
318 other MODIS data products.

For the continental-scale estimation of NEE, we obtained continental-scale MODIS data including surface reflectance, daytime and nighttime LST, and EVI from the Earth Observing System (EOS) Data Gateway. For each variable and for each 8- or 16-day period, a total of 22 tiles were needed to cover the conterminous U. S., and these tiles were mosaiced to generate a continental-scale image. For each variable, we determined the quality of the value of each pixel using the QA flags, and replaced the bad-quality value using a linear interpolation approach (Zhao et al., 2005). The NDWI was calculated from band 2 (near-infrared, 841-876nm) and band 6 (shortwave infrared, 1628-1652) of the surface reflectance product (MOD09A1) according to equation (5). Each 16-day EVI composite was split into two 8-day composites to correspond with the compositing interval of other MODIS data products.

2.3.3. Land cover

To construct the predictive NEE model, we obtained the land cover type for each AmeriFlux site based on the site descriptions (Table 1), and categorized each site into a class of the University of Maryland land-cover classification system (UMD). Although the 42 AmeriFlux sites used in this study cover a variety of vegetation classes of this classification system, some classes had a minimal or no sites (n = 0-2). We therefore reclassified all vegetation classes of the UMD classification system to seven broader classes (Table 2). Specifically, evergreen needleleaf forests and evergreen broadleaf forests were merged to evergreen forests, deciduous needleleaf forests and deciduous broadleaf forests to deciduous forests, closed shrublands and open shrublands to shrublands, and woody savannas and savannas to savannas.

To estimate NEE for each 1 km × 1 km cell at the continental scale, we obtained the land cover type for each cell from the MODIS land cover map with the UMD classification

342 system (Friedl et al., 2002). Similarly, we reclassified the vegetation types of the MODIS land
343 cover map to the seven broader classes (Table 2). The reclassified land-cover map is shown in
344 Fig. 1.

345 2.4. *Model development*

346 We developed a predictive NEE model using Cubist based on the site-level MODIS
347 and AmeriFlux NEE data. Our explanatory variables included surface reflectance (7 bands),
348 daytime and nighttime LST, EVI, fPAR, and LAI, and our target variable was NEE. We split
349 the site-level data set of AmeriFlux and MODIS data into a training set (2000-2004) and a test
350 set (2005-2006). If a site only had NEE observations for the period 2000-2004, the site was
351 only included in the training set; if a site only had NEE observations for the period 2005-2006,
352 the site was only included in the test set; otherwise, the site was included in both training and
353 test sets. The training and test sets included 40 and 34 AmeriFlux sites, respectively.
354 Altogether we had a total of 4596 and 2257 data points for the training and test sets,
355 respectively. We trained the model with the training set, and tested the model with the test set
356 (2005-2006). In addition to the full model that includes all the 14 explanatory variables, we
357 also developed a series of models by dropping one or more variables at a time using Cubist. To
358 select the best model, we evaluated the performance of each model based on the average error,
359 relative error, and correlation coefficient. We chose the model with the minimal average error
360 and relative error and maximum correlation coefficient as the best model. We also evaluated
361 the model performance using scatterplots of predicted versus observed NEE and seasonal
362 variations between the predicted and observed NEE.

363 *2.5. Continental-scale estimation of NEE*

364 The AmeriFlux network is representative of the conterminous U.S. ecoregions
365 (Hargrove et al., 2003). The 42 sites used in this study included most of the active flux sites in
366 the network and cover a variety of vegetation types (Fig. 1, Table 1). Moreover, these sites
367 encompass typical U.S. climate types (Fig. 2). We believe that the predictive NEE model
368 constructed from the 42 sites can be extrapolated to the conterminous U.S. Thus, we applied
369 the predictive NEE model to estimate NEE for each 1 km × 1 km cell across the conterminous
370 U.S. for each 8-day period in 2005 using wall-to-wall MODIS data. We then examined the
371 spatiotemporal patterns of our NEE estimates.

372 **3. Results and discussion**

373 *3.1. Model development*

374 The best model contained the following explanatory variables, including surface
375 reflectance bands 1-6, EVI, daytime and nighttime LST, and NDWI (relative error = 0.64,
376 average error = 0.986, r = 0.73). This model achieved slightly higher performance than the full
377 model (relative error = 0.66, average error = 1.01, r = 0.72). The best model estimated NEE
378 reasonably well (Fig. 3) considering that we used multiple years of data from a number of sites
379 involving a variety of vegetation types across the conterminous U.S. The model slightly
380 underestimated positive NEE values, and overestimated negative NEE values, where negative
381 values indicate carbon uptake, and positive values indicate carbon release. In absolute
382 magnitudes, the model slightly underestimated both carbon release and uptake rates, thus
383 damping the observed amplitude.

384 [insert Fig. 3 about here]

385 The analysis of NEE residuals (Fig. 4) indicated that the residuals were not randomly
386 distributed. In absolute magnitudes, low NEE values were generally associated with low

prediction errors, whereas high NEE values were associated with high prediction errors. This indicated that the explanatory variables included in the model could not completely explain the variance of NEE. For example, the independent variables used in the model could not account for the sizes of soil organic carbon pools and the effects of disturbances, thereby affecting the performance of the model for estimating NEE.

[insert Fig. 4 about here]

We calculated the average error and relative error across all AmeriFlux sites for each 8-day period, and then plotted these two types of error against time (Fig. 5). The average error showed a strong seasonality. In absolute magnitudes, winter had low average errors (~0.6 g C m^{-2} day^{-1}), whereas warm season errors often exceeded 1 g C m^{-2} day^{-1}. This suggests the relatively large uncertainties associated with NEE estimates, indicating that random errors in NEE measurements are substantial (Richardson et al., 2008), and these errors ultimately limit the agreement between observed and predicted NEE values.

[insert Fig. 5 about here]

We also compared our NEE estimates with observed NEE for each AmeriFlux site (Fig. 6). The NEE estimates captured most features of observed NEE such as seasonality and interannual variability over the period 2005-2006. For some sites, episodes of under- or over-prediction occurred. The model could not capture exceptionally high and low NEE values that represented large carbon release and uptake rates, respectively for some sites (e.g., the Audubon Research Ranch site (AZ), Fermi National Accelerator Laboratory Agricultural site (IL), Goodwin Creek site (MS), and Fort Peck (MT)). In absolute magnitudes, the model substantially underestimated those exceptional values. For example, the model estimates were far below the observed NEE values that were greater than 2 g C m^{-2} day^{-1} at the Goodwin

410 Creek site (MS), and were far above the observed NEE values below -3 g C m^{-2} day^{-1} at the
411 Audubon Research Ranch site (AZ). Overall, the model performed better for deciduous forests,
412 savannas, grasslands and croplands than for evergreen forests and shrublands.
413 [insert Fig. 6 about here]
414 The disagreement between estimated and observed NEE values is likely due to the
415 following reasons. First, the MODIS and tower footprints do not always match with each other.
416 As mentioned earlier, for each explanatory variable derived from MODIS data, we used the
417 values averaged within the 3 km × 3 km area (i.e., MODIS footprint) surrounding each flux
418 tower to represent the values of the tower site. The footprints of MODIS and AmeriFlux
419 matched with each other for most sites because the vegetation structure within the 3 km × 3 km
420 area surrounding the flux tower is similar to that at the tower. However, some sites are located
421 in complex land mosaics, and the vegetation structure at the flux tower could be significantly
422 different from that within the MODIS footprint. For example, the Tonzi Ranch site (CA) is
423 dominated by deciduous blue oaks (*Quercus douglasii*), and the understory and open grassland
424 are dominated by cool-season C_3 annual species (Ma et al., 2007). The MODIS footprint,
425 however, consists of a larger fraction of grassland. The phenologies of blue oaks and grassland
426 are distinct from each other (Ma et al., 2007), and therefore these two plant species had
427 differential contributions to the NEE integrated over the MODIS footprint. In the spring, wet
428 conditions along with warm temperatures facilitated the fast growth of grass, leading to large
429 carbon uptake rates within the MODIS footprint. As a result, in absolute magnitudes, our NEE
430 estimates were higher than the observed values at the tower site. Grasses senesced by the end
431 of the spring as the rainy season ended (Ma et al., 2007). The senescence of grasses led to
432 carbon release in the summer, and thus lowered the carbon uptake rates integrated over the

MODIS footprint. Therefore, in absolute magnitudes, our NEE values were much lower than the observed values at the tower in the summer.

Second, some sites experienced substantial disturbances that alter ecosystem carbon fluxes. For example, the Austin Cary site (FL) suffered from an extreme drought over the period 1999-2002; a prescribed burn at the site in 2003 removed 95% of the understory vegetation. The site was also hit by three hurricanes in 2004. These disturbances reduced carbon uptake rates, whereas MODIS data are less sensitive to changes in understory vegetation in forest ecosystems, thereby leading to substantial overestimation of carbon uptake rates.

Third, our model could not sufficiently account for the factors influencing R_H. As mentioned earlier, R_H is influenced by substrate availability, soil temperature, and soil moisture. LST and NDWI can account for soil temperature and soil moisture. However, surface reflectance can only partly account for non-photosynthetic material (e.g., litter). Root and associated mycorrhizal respiration produce roughly half of soil respiration, with much of the remainder derived from decomposition of recently produced root and leaf litter (Ryan and Law, 2005). Changes in the carbon stored in the soil generally contribute little to soil respiration, but these changes, together with shifts in plant carbon allocation, determine ecosystem carbon storage belowground and its exchange with the atmosphere (Ryan and Law, 2005). The incapability of our model to account for transient carbon pools contributed to the uncertainties in the NEE estimates (Richardson et al., 2007).

Finally, we estimated NEE for 8-day interval, and therefore our estimates could not capture the variability of NEE within the interval. The MODIS LST and EVI products were averaged from the corresponding daily products over a period of 8 and 16 days, respectively

(Huete et al., 2002; Wan et al., 2002). For each period, only data with good quality were retained for compositing, and thus the number of days actually used for compositing is often lower than the total number of days over the period. The compositing technique for the MODIS surface reflectance product is based on the minimum-blue criterion that selects the clearest conditions over the 8-day period (Vermote and Vermeulen, 1999). Therefore, the 8- or 16-day values do not always represent the average environmental conditions and average fluxes over the 8- or 16-day period. The exclusion of days with high and low values could lead to underestimation and overestimation of NEE values, respectively. For example, each 16-day EVI composite was an average of daily EVI over a period of 16 days. The number of acceptable pixels over a 16-day compositing period is typically less than 10 (often less than 5) due to cloud contaminations and extreme off-nadir sensor view angles (Huete et al., 2002). The compositing process may exclude high EVI values that represented high fPAR or fractional vegetation cover, therefore leading to lower carbon uptake rates. On the other hand, the compositing process may also exclude low EVI values that represented low fPAR or fractional vegetation cover, thereby leading to higher carbon uptake rates. Sims et al. (2005) suggested that midday GPP derived from daily satellite snapshots of vegetation was highly correlated with 8-day mean GPP, and the inclusion of cloudy days within 8-day intervals had less effect on daily GPP than expected. However, the exclusion of cloudy days may have a larger impact on R_e, leading to a large impact on NEE.

[insert Fig. 7 about here]

We averaged the estimated and observed 8-day NEE for each AmeriFlux site and examined the relationship between the estimated and observed mean 8-day NEE across the sites (Fig. 7). The model estimated NEE reasonably well at the site level ($r^2 = 0.72$, $p <$

0.00001). Overall, in absolute magnitudes, the model underestimated NEE. The performance of the model also varied with site. On average, some sites were carbon sources, whereas other sites were carbon sinks. Large overestimation of carbon uptake occurred at the Toledo Oak Openings site (OH), whereas large underestimation of carbon uptake occurred at the Mature Red Pine site (WI), Duke Forest Pine site (NC), Duke Forest Hardwoods (NC), and North Carolina Pine (NC). Large overestimation of carbon release occurred at Audubon Research Ranch (AZ), ARM Oklahoma (OK), and Freeman Ranch Mesquite (TX), whereas large underestimation of carbon release occurred at Mead Irrigated (NE), Goodwin Creek (MS), and Austin Cary (FL).

[insert Fig. 8 about here]

We also averaged our estimated and observed 8-day NEE over all AmeriFlux sites for each vegetation type (i.e., biome), and examined the relationship between estimated and observed NEE across the vegetation types (Fig. 8). The model predicted NEE at the biome level very well ($r^2 = 0.95$, $p < 0.00001$). Again, in absolute magnitudes, the model underestimated NEE. The performance of the model also varied with vegetation type. In absolute magnitudes, large overestimation occurred for evergreen forests and shrublands.

Our study demonstrated that MODIS data have great potential for scaling up flux tower NEE data to continental scales across a variety of vegetation types. Unlike GPP (Heinsch et al., 2006; Yang et al., 2007), NEE is much more difficult to estimate because the transient carbon pools and associated heterotrophic respiration are difficult to estimate (Running et al., 2004). The performance of our model for estimating NEE is remarkable, given the diversity in ecosystem types, age structures, fire and insect disturbances, and management practices. In future research, additional explanatory variables should be selected to better account for live

and dead vegetation carbon pools, and other factors that influence decomposition of woody detritus and soil respiration.

3.2. Continental-scale estimation of NEE

We estimated NEE for each 1 km × 1 km cell across the conterminous U.S. for each 8-day interval over the period 1/1/2005-2/28/2006. Fig. 9 shows examples of 8-day NEE maps that we produced for the conterminous U.S. from January through February. For each month, the second 8-day NEE map was shown here. The predictive model trained at the AmeriFlux sites generally captured the expected spatiotemporal patterns of NEE. The majority of the conterminous U.S. released carbon or were nearly carbon neutral in winter months because at this time of the year the canopies of most ecosystems were dormant; in summer months, ecosystems in the East assimilated carbon from the atmosphere, whereas many areas in the west released carbon, possibly due to summer drought effects on NEE, although the severity of drought was the greatest in August to September. In fall months, ecosystems in the East assimilated less carbon than in the summer months as vegetation began to senesce. Some ecosystems, particularly evergreen forests in the Pacific Northwest and California, assimilated carbon from the atmosphere throughout the year. Douglas-fir, a major species in the Pacific Northwest and California, is known to be highly plastic and able to photosynthesize in winter when temperatures are above freezing.

[insert Fig. 9 about here]

We aggregated 8-day NEE estimates for each season in 2005 (Fig. 10). Our NEE estimates exhibited strong seasonal fluctuations, agreeing with previous studies (e.g., Falge et al., 2002). The NEE estimates also varied substantially over space. In the spring, many areas in the eastern half of the conterminous U.S. including the Southeast and the Gulf Coast

assimilated carbon from the atmosphere. The growing season of these ecosystems started in the mid- to late spring, and GPP quickly exceeded R_e, leading to net carbon uptake in the season. By contrast, the Upper Great Lakes region, the northern Great Plains, and the New England region assimilated carbon. The Upper Great Lakes region and the northern Great Plains are dominated by croplands with most crops planted between April-June (corn planted between April and mid-May; soybeans between mid-May and mid-June; and sorghum between late May and late June; Shroyer et al., 1996). Crops were sparse in the beginning of the growing season and R_e exceeded GPP, thereby leading to carbon releases. The New England region and the northern portion of the Upper Great Lakes region are dominated by temperate-boreal transitional forests, and their relatively late greenup due to low air temperatures led to carbon releases in the spring. Many regions in the western half of the conterminous U. S. released carbon in the spring because of the sparse vegetation and the dominance of R_e over GPP. The Pacific Coast assimilated carbon even in the spring because the dominant evergreen forests in the region assimilated carbon due to mild temperatures and moist conditions (Anthoni et al., 2002). The Mediterranean regions in California also assimilated carbon in the spring. The Mediterranean climate is characterized by mild winter temperatures concomitant with the rainy season as opposed to severe summer droughts and heat (Barbour and Minnich, 2000). These ecosystems assimilated carbon because of precipitation surplus and relatively warm temperatures in the spring (Xu and Baldocchi, 2004; Ma et al., 2007).

[insert Fig. 10 about here]

In the summer months, the eastern half of the conterminous U.S. assimilated carbon because GPP far exceeded R_e owing to favorable temperature and soil moisture conditions. By contrast, a vast majority of the land across the western counterpart released carbon, including

548 the Great Basin, the Colorado Plateau, and the western Great Plains. The 2005 summer drought
549 affected these regions (National Climatic Data Center, 2008) and reduced GPP, whereas the
550 high temperatures increased R_e, leading to net carbon releases. Some other regions in the West
551 also assimilated carbon, including the northern Rocky Mountains and the Pacific Coast. Some
552 Mediterranean ecosystems in California also released carbon due to precipitation deficits in the
553 summer.

554 In the fall, the Southeast and the Gulf Coast still assimilated carbon, but net carbon
555 uptake rates substantially decreased relative to those in the summer. This is because vegetation
556 began to senesce in these regions in the fall. The Upper Great Lakes region and the Great
557 Plains largely released carbon due to the harvesting of crops. The majority of the land across
558 the west including the Great Plains, the Great Basin, and the Colorado Plateau released carbon.
559 The northern Pacific Coast, however, still absorbed carbon. The Mediterranean ecosystems in
560 California continued releasing carbon as the dry season spanned into the fall.

561 In the winter, the vast majority of the conterminous U.S. released carbon as the
562 canopies of most ecosystems were dormant at this season of the year. Some regions in the
563 Pacific Coast, however, assimilated carbon even in the winter because of the dominance of
564 evergreen forests and mild temperatures in the regions (Waring and Franklin, 1979). This
565 agreed with the finding of Anthoni et al. (2002) that old-growth ponderosa pine in Oregon
566 slightly assimilated carbon in the winter season. For the Mediterranean ecosystems in
567 California, a smaller part of the region released carbon into the atmosphere relative to the fall
568 as the wet season started in the winter.

569 [insert Fig. 11 about here]

570 The trajectory of the mean 8-day NEE (g C m^{-2} day^{-1}) for each vegetation type
571 averaged over the entire conterminous U.S. throughout 2005 (Fig. 11a) showed that deciduous
572 forests, croplands, savannas, and mixed forests had large intra-annual variability in NEE,
573 whereas evergreen forests, grasslands, and shrublands exhibited much less interannual
574 variability. The seasonal patterns of NEE were determined by the seasonal differences in LAI,
575 physiological capacity, meteorological conditions, growing season length, soil temperature,
576 moisture status, and management practices (Falge et al., 2002). In the late fall, winter, and
577 early spring, on average, the U.S. terrestrial ecosystems released carbon. Taken separately,
578 only evergreen forests and grasslands assimilated carbon. Among vegetation types exhibiting
579 positive NEE values, deciduous forests had the highest values, followed by mixed forests;
580 croplands exhibited intermediate values; shrublands and savannas exhibited lowest values
581 while evergreen forests still assimilated carbon. During the growing season, on average, the
582 U.S. terrestrial ecosystems strongly assimilated carbon. Taken separately, only shrublands
583 released carbon because of high temperatures and low soil moisture conditions. Among
584 vegetation types assimilating carbon, the highest absorption rates occurred for deciduous
585 forests, followed by croplands, savannas, and mixed forests; intermediate rates occurred for
586 evergreen forests; the lowest rates occurred for grasslands. Baldocchi et al. (2001) showed that
587 the net CO_2 exchange of temperate deciduous forests increases by about 5.7 g C m^2 day^{-1} for
588 each additional day that the growing season, defined as the period over which mean daily CO_2
589 exchange is negative due to net uptake by ecosystems, is extended. We found that on average,
590 the CO_2 exchange of deciduous and evergreen forests across the conterminous U.S. increased
591 3.6 and 1.2 g C m^{-2} day^{-1} for each additional day that the growing season is extended,
592 respectively. Our continental-scale estimate for deciduous forests was 37% lower than that

593 estimated by Baldocchi et al. (2001) likely because our estimate was based on all the areas
594 covered by deciduous forests encompassing the full range of productivity.

595 The trajectory of the total 8-day NEE (Tg C day^{-1}) aggregated from the NEE estimates
596 over the conterminous U.S. (Fig. 11b) showed clear dependence on vegetation type. The
597 differences in the trajectories of total 8-day NEE among vegetation types were different from
598 those of mean 8-day NEE because of the differences in the areas among vegetation types
599 (Figure 11b). In the late fall, winter, and early spring, the U.S. terrestrial ecosystems released
600 carbon (1-2 Tg C day^{-1}). Taken separately, croplands, deciduous forests, and mixed forests
601 released carbon, whereas evergreen forests assimilated carbon; shrublands, savannas, and
602 grasslands, however, were nearly carbon neutral. During the growing season, the U.S.
603 terrestrial ecosystems assimilated carbon, with peak total NEE of -17 Tg C day^{-1}. All
604 vegetation types except shrublands assimilated carbon. In absolute magnitudes, the highest
605 total NEE ($\approx$ 10 Tg C day^{-1}) occurred for croplands; the intermediate values occurred for
606 deciduous forests, savannas, and mixed forests; the lowest values occurred for evergreen
607 forests and grasslands. By contrast, shrublands released carbon. Total 8-day NEE also showed
608 largest intra-annual variability for croplands, intermediate variability for deciduous forests,
609 savannas, and mixed forests, and lowest variability for evergreen forests, grasslands, and
610 shrublands.

611 **4. Summary and conclusions**

612 We combined MODIS and NEE data from 42 AmeriFlux sites involving a variety of
613 vegetation types to develop a predictive NEE model using a regression tree approach. The
614 model was trained and validated using NEE data over the periods 2000-2004 and 2005-2006,
615 respectively. The model estimated NEE at the site level reasonably well. We then applied the

616 model to estimate NEE for each 1 km × 1 km cell across the conterminous U.S. for each 8-day
617 period in 2005. The model generally captured the expected spatial and seasonal patterns of
618 NEE. Our study demonstrated that our empirical approach along with MODIS data have great
619 potential for scaling up AmeriFlux NEE measurements to the continental scale.

620 Our wall-to-wall NEE estimates across the conterminous U.S. provided an independent
621 dataset from simulations by biogeochemical modeling and inverse modeling for examining the
622 spatiotemporal patterns of NEE and constraining U.S. terrestrial carbon sinks/sources. Our
623 estimates have advantages over these models simulations by taking advantage of NEE
624 measurements from a number of AmeriFlux sites involving representative U.S. ecosystems.
625 Our scaling-up approach implicitly considered the effects of climate variability and extreme
626 climate events. Disturbances such as wildfires, hurricanes, and insect defoliation significantly
627 affect ecosystem carbon fluxes (e.g., Thornton et al., 2002). Although our NEE estimates could
628 not capture the immediate emissions of CO_2 due to the burning of biomass in wildfires and
629 logging, our estimates could partly account for the carbon fluxes following the disturbances
630 because the MODIS data we used provide real-time observations of ecosystems. Compared to
631 inverse modeling techniques, our approach provided estimates at high spatial (1 km × 1 km)
632 and temporal resolutions (8 day). In addition, NEE is notoriously difficult to quantify over
633 large areas (Running et al., 2004), and the accuracy of simulated NEE for regions and
634 continents by biogeochemical models is poorly known due to lack of spatially explicit,
635 independent validation datasets. Our estimates may also provide an independent validation
636 dataset for these model simulations.

637 The AmeriFlux sites provide valuable measurements of ecosystem carbon exchange for
638 examining terrestrial carbon dynamics (Law, 2006, 2007). Our study demonstrated that the

AmeriFlux measurements could be used to examine continental-scale carbon dynamics, and the continuing operation of the AmeriFlux network will continue to improve our understanding of the impacts of climate variability, disturbances, and management practices on terrestrial carbon cycling. Our study also suggested that the current AmeriFlux network should be augmented by establishing more sites for certain biomes in the UMD classification system (Table 1), including open shrublands, savannas, grasslands, and croplands. The augmentation will enable the differentiation of open shrublands from closed shrublands, woody savannas from savannas, and C_3 from C_4 plants in scaling-up studies, thereby improving the estimation of carbon fluxes for large areas.

Acknowledgements:

The work of J. Xiao and Q. Zhuang was partly funded by the National Science Foundation (NSF) Carbon and Water Program (EAR-0630319). We also thank the US Department of Energy Biological and Environmental Research, Terrestrial Carbon Program (Award #DE-FG02-04ER63917) for funding Dr. B. E. Law to develop the AmeriFlux network protocols and database design for the network, and the Office of Science, U.S. Department of Energy, through the Midwestern Regional Center of the National Institute for Global Environmental Change under Cooperative Agreements No. DE-FC03-90ER610100 for funding P. S. Curtis. We thank the principal investigators of the MODIS data products including A. R. Huete, Z. Wan, R. B. Myneni, and E. F. Vermote and other contributors as well as the Oak Ridge National Laboratory (ORNL) Distributed Active Archive Center (DACCC) and the Earth Observing System (EOS) Data Gateway for making these products available. We also thank T. A. Boden at the Carbon Dioxide Information Analysis Center,

ORNL, S. K. S. Vannan at the ORNL DACC, M. Zhao at the University of Montana, and Z. Wan at the University of California, Santa Barbara for helpful discussion about AmeriFlux data, MODIS ASCII subsets, MODIS Quality Assurance (QA) flags, and MODIS LST, respectively. Computing support was provided by the Rosen Center for Advanced Computing, Purdue University.

References:

AmeriFlux, 2007. AmeriFlux Network. http://public.ornl.gov/ameriflux/. Visited on 10/04/2007.

Anthoni, P.M., Unsworth, M.H., Law, B.E., Irvine, J., Baldocchi, D.D., Tuyl, S.V., Moore, D., 2002. Seasonal differences in carbon and water vapor exchange in young and old-growth ponderosa pine ecosystems. Agri. For. Meteor. 111, 203-222.

Asrar, G., Fuchs, M., Kanemasu, E.T., Hatfield, J.L., 1984. Estimating of absorbed photosynthesis radiation and leaf area index from spectral reflectance in wheat. Agron. J. 76, 300-306.

Baldocchi, D., Falge, E., Gu, L., Olson, R., Hollinger, D., Running, S., Anthoni, P., Bernhofer, C., Davis, K., Evans, R., Fuentes, J., Goldstein, A., Katul, G., Law, B., Lee, X., Malhi, Y., Meyers, T., Munger, W., Oechel, W., Paw U, K.T., Pilegaard, K., Schmid, H.P., Valentini, R., Verma, S., Vesala, T., Wilson, K., Wofsy, S., 2001. FLUXNET: A new tool to study the temporal and spatial variability of ecosystem-scale carbon dioxide, water vapor, and energy flux densities. Bull. Amer. Meteor. Soc. 82, 2415-2434.

Barbour, M., Minnich, B., 2000. California upland forests and woodlands, in *North American Terrestrial Vegetation, 2nd Editions*, edited by M. Barbour, and W. Billings, pp. 161-202, Cambridge Univ Press, Cambridge UK.

Belward, A.S., Estes, J.E., Kline, K.D., 1999. The IGBP-DIS Global 1-km Land-Cover Data Set DISCover: A Project Overview. Photogram. Eng. Remote Sens. 65, 1013-1020.

Breiman, L., Friedman, J., Olshen, R., Stone, C., 1984. *Classification and regression trees*. Chapman and Hall, New York, 358pp.

Ceccato, P., Gobron, N., Flasse, S., Pinty, B., Tarantola, S., 2002. Designing a spectral index to estimate vegetation water content from remote sensing data: Part 1 - Theoretical approach. Remote Sen. Environ. 82, 188-197.

Chen, J, Brosofske, K.D., Noormets, A., Crow, T.R., Bresee, M.K., Le Moine, J.M., Euskirchen, E.S., Mather, S.V., Zheng, D., 2004. A working framework for quantifying carbon sequestration in disturbed land mosaics. Environ. Manage. 34, S210-221.

Clark, K.L., Gholz, H.L., Moncrieff, J.B., Cropley, F., Loescher, H.W., 1999. Environmental controls over net carbon dioxide from contrasting Florida ecosystems. Ecol. App. 9, 936-948.

Clark, K.L., Gholz, H.L., Castro, M.S., 2004. Carbon dynamics along a chronosequence of slash pine plantations in N. Florida. Ecol. App. 4, 1154-1171.

Cook, B.D., Davis, K.J., Wang, W., Desai, A., Berger, B.W., Teclaw, R.M., Martin, J.G., Bolstad, P.V., Bakwin, P.S., Yi, C., Heilman, W., 2004. Carbon exchange and venting anomalies in an upland deciduous forest in northern Wisconsin, USA. Agri. For. Meteor. 126, 271-295.

DeFries, R.S., Houghton, R.A., Hansen, M. C., Field, C. B., Skole, D., Townshend, J., 2002. Carbon emissions from tropical deforestation and regrowth based on satellite observations for the 1980s and 1990s. PNAS 99, 14256-14261.

Deng, F., Chen, J.M., Ishizawa, M., Yuen, C-W., Mo, G., Higuchi, K., Chan, D., Maksyutov, S., 2007. Global monthly CO_2 flux inversion with a focus over North America. Tellus 59B, 179-190.

Denning, A.S., Gollatz, J.G., Zhang, C., Randall, D.A., Berry, J.A., Sellers, P.J., Colello, G.D., Dazlich, D.A., 1996. Simulations of terrestrial carbon metabolism and atmospheric CO_2 in a general circulation model. Part 1: Surface carbon fluxes. Tellus 48B, 521-542.

731 Desai, A.R., Bolstad, P.V., Cook, B.D., Davis, K.J., Carey, E.V., 2005. Comparing net
732 ecosystem exchange of carbon dioxide between an old-growth and mature forest in the
733 upper Midwest, USA. Agri. For. Meteor. 128, 33-55.
734 Dore, S., Hymus, G.J., Johnson, D.P., Hinkle, C.R., Valentini, R., Drake, B.G., 2003. Cross
735 validation of open-top chamber and eddy covariance measurements of ecosystem CO2
736 exchange in a Florida scrub-oak ecosystem. Global Change Biol. 9, 84-95.
737 Falge, E., Baldocchi, D., Olson, R., Anthoni, P., Aubinet, M., Bernhofer, C., Burba,
738 G., Ceulemans, R., Clement, R., Dolman, H., Granier, A., Gross, P., Grunwald,
739 T., Hollinger, D., Jensen, N.-O., Katul, G., Keronen, P., Kowalski, A., Lai, C.T., Law,
740 B.E., Meyers, T., Moncrieff, J., Moors, E., Munger, J.W., Pilegaard, K., Rannik,
741 U., Rebmann, C., Suyker, A., Tenhunen, J., Tu, K., Verma, S., Vesala, T., Wilson,
742 K., Wofsy, S, 2001. Gap filling strategies for defensible annual sums of net ecosystem
743 exchange. Agri. For. Meteor. 107, 43-69.
744 Falge, E., Baldocchi, D., Tenhunen, J., Aubinet, M., Bakwin, P., Berbigier, P., Bernhofer, C.,
745 Burba, G., Clement, R., Davis, K.J., Elbers, J.A., Goldstein, A.H., Grelle, A., Granier, A.,
746 Guðmundsson, J., Hollinger, D., Kowalski, A.S., Katul, G., Law, B.E., Malhi, Y., Meyers,
747 T., Monson, R.K., Munger, J.W., Oechel, W., Paw U, K.T., Pilegaard, K., Rannik, U.,
748 Rebmann, C., Suyker, A., Valentini, R., Wilson, K., Wofsy, S., 2002. Seasonality of
749 ecosystem respiration and gross primary production as derived from FLUXNET
750 measurements. Agri. For. Meteor. 113, 53-74.
751 Falk, M., Wharton, S., Schroeder, M., Ustin, S., Paw U, K.T., 2008. Flux partitioning in an
752 old-growth forest: seasonal and interannual dynamics. Tree Physiol. 28, 509-520.

753 Fan, S. M., Gloor, M., Mahlman, J., Pacala, S., Sarmiento, J., Takahashi, T., Tans, P., 1998. A
754 large terrestrial carbon sink in North America implied by atmospheric and oceanic carbon
755 dioxide data and models. Science 282, 442-446.
756 Fensholt, R., Sandholt, I., 2003. Derivation of a shortwave infrared water stress index from
757 MODIS near- and shortwave infrared data in a semiarid environment. Remote Sens.
758 Environ. 87, 111-121.
759 Field, C.B., Randerson, J.T., Malmstrom, C.M., 1995. Global net primary production:
760 combining ecology and remote sensing. Remote Sens. Environ. 51, 74-88.
761 FLUXNET, 2008. FLUXNET Project. http://daac.ornl.gov/FLUXNET. Visited on 01/02/2008.
762 Friedl, M.A., McIver, D.K., Hodges, J.C.F., Zhang, X.Y., Muchoney, D., Strahler, A.H.,
763 Woodcock, C.E., Gopal, S., Schneider, A., Cooper, A., Baccini, A., Gao, F., Schaaf, C.,
764 2002. Global land cover mapping from MODIS: algorithms and early results. Remote Sens.
765 Environ. 83, 287-302.
766 Gao, B.C., 1996. NDWI - A normalized difference water index for remote sensing of
767 vegetation liquid water from space. Remote Sens. Environ. 58, 257-266.
768 Gough, C.M., Vogel, C.S., Schmid, H.P., Su, H-B., Curtis, P.S., 2008. Multi-year convergence
769 of biometric and meteorological estimates of forest carbon storage. Agri. For. Meteor. 148,
770 158-170.
771 Gu, L., Meyers, T., Pallardy, S.G., Hanson, P.J., Yang, B., Heuer, M., Hosman, K.P., Liu, Q.
772 Riggs, J.S., Sluss, D., Wullschleger, S.D., 2007. Influences of biomass heat and
773 biochemical energy storages on the land surface fluxes and radiative temperature. J.
774 Geophys. Res. D02107, doi:10.1029/2006JD007425.

775 Gu, L., Meyers, T., Pallardy, S.G., Hanson, P.J., Yang, B., Heuer, M., Hosman, K.P., Riggs,
776 J.S., Sluss, D., Wullschleger, S.D., 2006. Direct and indirect effects of atmospheric
777 conditions and soil moisture on surface energy partitioning revealed by a prolonged
778 drought at a temperate forest site. J. Geophys. Res. D16102, doi:10.1029/2006JD007161.
779 Gurney, K.R., Law, R.M., Denning, A.S, Rayner, P.J., Baker, D., Bousquet, P., Bruhwiler, L.,
780 Chen, Y-H., Ciasi, P., Fan, S., Fung, I.Y., Gloor, M., Heimann, M., Higuchi, K., John, J.,
781 Maki, T., Maksyutov, S., Masarie, K., Peylin, P., Prather, M., Pak, B.C., Randerson, J.,
782 Sarmiento, J., Taguchi, S., Takahashi, T., Yuen, C-W., 2002. Towards robust regional
783 estimates of CO_2 sources and sinks using atmospheric transport models. Nature 415, 626-
784 630.
785 Hargrove, W. W., Hoffman, F. M., Law, B. E., 2003. New analysis reveals representativeness
786 of the AmeriFlux network. EOS Trans. AGU, 84, 529-544.
787 Heinsch, F. A., Zhao, M., Running, S.W., Kimball, J.S., Nemani, R.R., Davis, K.J., Bolstad,
788 P.V., Cook, B.D., Desai, A.R., Ricciuto, D.M., Law, B.E., Oechel, W.C., Kwon, H.J., Luo,
789 H., Wofsy, S.C., Dunn, A.L., Munger, J.W., Baldocchi, D.D., Xu, L., Hollinger, D.Y.,
790 Richardson, A.D., Stoy, P.C., Siqueira, M.B.S., Monson, R.K., Burns, S.P., and Flanagan,
791 L.B., 2006. Evaluation of remote sensing based terrestrial productivity from MODIS using
792 regional tower eddy flux network observations. IEEE Trans. Geosci. Remote Sens. 44,
793 1908-1925.
794 Hollinger, D.Y., Goltz, S.M., Davidson, E.A., Lee, J.T., Tu, K.,
795 Valentine, H.T., 1999. Seasonal patterns and environmental control of carbon
796 dioxide and water vapor exchange in an ecotonal boreal forest. Global
797 Change Biol. 5, 891-902

798 Hollinger, D.Y., Aber, J., Dail, B., Davidson, E.A., Goltz, S.M., Hughes, H., Leclerc, M.
799 Y., Lee, J.T., Richardson, A.D., Rodrigues, C., Scott, N.A.,
800 Achuatavarier, D., Walsh, J., 2004. Spatial and temporal variability in
801 forest-atmosphere CO_2 exchange. Global Change Biol. 10, 1689-1706.
802 Hollinger, S.E., Bernacchi, C.J., Meyers, T.P., 2005. Carbon budget of mature no-till
803 ecosystem in North Central Region of the United States. Agri. For. Meteor. 130, 59-69,
804 2005.
805 Huang, C., Townshend, J.R.G., 2003. A stepwise regression tree for nonlinear approximation:
806 applications to estimating subpixel land cover. Int. J. Remote Sens. 24, 75-90.
807 Huete, A.R., Liu, H.Q., Batchily, K., vanLeeuwen, W., 1997. A comparison of vegetation
808 indices global set of TM images for EOS-MODIS. Remote Sens. Environ. 59, 440-451.
809 Huete, A., Didan, K., Miura, T., Rodriguez, E.P., Gao, X., Ferreira, L.G., 2002. Overview of
810 the radiometric and biophysical performance of the MODIS vegetation indices. Remote
811 Sens. Environ. 83, 195-213.
812 Hunt, E.R., Rock, B.N., 1989. Detection of changes in leaf water content using near and
813 middle-infrared reflectances Remote Sens. Environ. 30, 43–54.
814 Irvine, J., Law, B.E., Hibbard, K.A., 2007. Postfire carbon pools and fluxes in semiarid
815 ponderosa pine in Central Oregon. Global Change Biol. 13, 1748-1760.
816 Jackson, T. J., Chen, D., Cosh, M., Li, F., Anderson, M., Walthall, C., Doriaswamy, P., Hunt,
817 E.R., 2004. Vegetation water content mapping using Landsat data derived normalized
818 difference water index fro corn and soybeans. Remote Sens. Environ. 92, 475-482.
819 Jenkins, J.P., Richardson, A.D., Braswell, B.H., Ollinger, S.V., Hollinger, D.Y., Smith, M.-L.,
820 2007. Refining light-use efficiency calculations for a deciduous forest canopy using

821 simultaneous tower-based carbon flux and radiometric measurementsk. Agri. For. Meteor.
822 143, 64-79.
823 Janssens, I.A., Freibauer, A., Ciais, P., Smith, P., Jabuurs, G-J. et al., 2003. Europe's terrestrial
824 biosphere absorbs 7 to 12% of European anthropogenic CO_2 emissions. Science 300, 1538-
825 1542.
826 Law, B.E., 2006. Carbon dynamics in response to climate and disturbance: recent progress
827 from multiscale measurements and modeling in AmeriFlux. In S. Yamamoto, ed. Plant
828 Responses to Air Pollution and Global Change. Springer, Tokyo, Japan.
829 Law, B.E., 2007. AmeriFlux network aids global synthesis. EOS Transactions 88, 286.
830 Law, B.E., Ryan, M.G., Anthoni, P.M., 1999. Seasonal and annual respiration of a ponderosa
831 pine ecosystem. Global Change Biol. 5, 169-182.
832 Law, B.E., Sun, O.J., Campbell, J., Tuyl, S.V., Thornton, P.E., 2003. Changes in carbon
833 storage and fluxes in a chronosequence of ponderosa pine. Global Change Biol. 9, 510-524.
834 Law, B.E., Turner, D., Campbell, J., Sun, O. J., Van Tuyl, S., Ritts, W. D., Cohen, W. B.,
835 2004. Disturbance and climate effects on carbon stocks and fluxes across Western Oregon
836 USA*, Global Change Biol. 10,* 1429-1444.
837 Law, B.E., Turner, D., Lefsky, M., Campbell, J., Guzy, M., Sun, O., Van Tuyl, S., Cohen, W.,
838 2006. Carbon fluxes across regions: Observational constraints at multiple scales. In J. Wu,
839 B. Jones, H. Li, O. Loucks, eds. *Scaling and Uncertainty Analysis in Ecology: Methods*
840 *and Applications*. Springer, USA. Pages 167-190.
841 Law, B.E., Waring, R.H., 1994, Remote sensing of leaf area index and radiation intercepted by
842 understory vegetation. Ecol. App. 4, 272-279.

Lipson, D.A., Wilson, R.F., Oechel, W.C., 2005. Effects of Elevated Atmospheric CO_2 on Soil Microbial Biomass, Activity, and Diversity in a Chaparral Ecosystem. App. Environ. Microbiol. 71, 8573-8580.

Ma, S., Baldocchi, D.D., Xu, L., Hehn, T., 2007. Inter-annual variability in carbon dioxide exchange of an oak/grass savanna and open grassland in California. Agri. For. Meteor. 147, 157-171.

Magnani, F., Mencuccini, M., Borghetti, M., Berbigier, P., Berninger, F. et al., 2007. The human footprint in the carbon cycle of temperate and boreal forests. Nature 447, 849-851.

Mahadevan, P., Wofsy, S.C., Matross, D.M., Xiao, X., Dunn, A.L., Lin, J.C., Gerbig, C., Munger, J.W., Chow, V.Y., Gottlieb, E.W., 2008. A satellite-based biosphere parameterization for net ecosystem CO_2 exchange: vegetation photosynthesis and respiration model (VPRM). Global Biogeochem. Cyc. doi:10.1029/2006GB002735, in press.

McGuire, A.D., Sitch, S., Clein, J.S., Dargaville, R., Esser, G., Foley, J., Heimann, M., Joos, F., Kaplan, J., Kicklighter, D. W., Meier, R.A., Melillo, J.M., Moore III, B., Prentice, I.C., Ramankutty, N., Reichenau, T., Schloss, A., Tian, H., Williams, L.J., Wittenberg, U., 2001. Carbon balance of the terrestrial biosphere in the twentieth century: analyses of CO_2, climate and land-use effects with four process-based ecosystem models. Global Biogeochem. Cyc. 15, 183-206.

Monson, R.K., Turnipseed, A.A., Sparks, J.P., Harley, P.C., Scott-Denton, L.E., Sparks, K., Huxman, T.E., 2002. Carbon sequestration in a high-elevation, subalpine forest. Global Change Biol. 8, 459-478.

865 Moffat, A.M., Papale, D., Reichstein, M., Hollinger, D.Y., Richardson, A.D., Barr, A.G.,
866 Beckstein, C., Braswell, B.H., Churkina, G., Desai, A.R., Falge, E., Gove, J.H., Heimann,
867 M., Hui, D., Jarvis, A.J., Kattge, J., Noormets, A., Stauch, V.J., 2007. Comprehensive
868 comparison of gap-filling techniques for eddy covariance net carbon fluxes. Agri. For.
869 Meteor. 147, 209-232.
870 Myneni, R.B., Dong, J., Tucker, C.J., Kaufmann, R.K., Kauppi, P.E., Liski, J., Zhou, L.,
871 Alexeyev, V., Hughes, M.K., 2001. A large carbon sink in the woody biomass of northern
872 forests. PNAS 98, 14784-14789.
873 Myneni, R.B., Hoffman, S., Knyazikhin, Y., Privette, J.L., Tian, Y., Wang, Y., Song, X.,
874 Zhang, Y., Smith, G.R., Lotsch, A., Friedl, M., Morisette, J.T., Votava, P., Nemani, R.R.,
875 Running, S.W., 2002. Global products of vegetation leaf area and fraction absorbed PAR
876 from year one of MODIS data. Remote Sens. Environ. 83, 214-231.
877 National Climatic Data Cneter, 2008. http://lwf.ncdc.noaa.gov/oa/climate/research/2005/persp
878 ectives.html, visited on 01/28/2008.
879 Nadelhoffer, K.J., Emmett, B.A., Gundersen, P., Kjønaas, O.J., Koopmans, C.J., Schleppi, P.,
880 Tietema, A., Wright, R.F., 1999. Nitrogen deposition makes a minor contribution to carbon
881 sequestration in temperate forests. Nature 398, 145–148.
882 Oak Ridge National Laboratory Distributed Active Archive Center (ORNL DAAC), 2006.
883 MODIS subsetted land products, Collection 4. Available on-line
884 (http://www.daac.ornl.gov/MODIS/modis.html) from ORNL DAAC, Oak Ridge,
885 Tennessee, U.S.A. Accessed Month 06, 2007.
886 Oren, R., Hsieh, C.-I., Stoy, P., Albertson, J., McCarthy, H.R., Harrell, P., Katul, G.G., 2006.
887 Estimating the uncertainty in annual net ecosystem carbon exchange: spatial variation in

888 turbulent fluxes and sampling errors in eddy-covariance measurements. Global Change
889 Biol. 12, 883-896.
890 Oren, R., Ewers, B.E., Todd, P., Phillips, N., Katul, G., 1998. Water balance delineates the soil
891 layer in which moisture affects canopy conductance. Ecol. App. 8, 990-1002.
892 Papale, D., Valentini, A., 2003. A new assessment of European forests carbon exchange by
893 eddy fluxes and artificial neural network spatialization. Global Change Biol. 9, 525-535.
894 Parton, W.J., Scurlock, J.M.O., Ojima, D.S., Gilmanov, T.G., Scholes, R.J., Schimel, D.S.,
895 Kirchner, T., Menaut, J.-C., Seastedt, T., Moya, E.G., Kamalrut, A., Kinyamario, J.I., 1993.
896 Observations and modeling of biomass and soil organic matter dynamics for the grassland
897 biome worldwide. Global Biogeochem. Cyc. 7, 785-809.
898 Pataki D.E., Oren, R., 2003. Species difference in stomatal control of water loss at the canopy
899 scale in a bottomland deciduous forest. Adv. Water Res. 26, 1267-1278.
900 Penuelas, J., Gamon, J.A., Griffin, K.L., Field, C.B., 1993. Assessing community type, plant
901 biomass, pigment composition, and photosynthetic efficiency of aquatic vegetation from
902 spectral reflectance. Remote Sens. Environ. 46, 110-118.
903 Potter, C.S., Randerson, J.T., Field, C.B., Matson, P.A., Vitousek, P.M., Mooney, H.A.,
904 Klosster, S.A., 1993. Terrestrial ecosystem production – a process model based on global
905 satellite and surface data. Global Biogeochem. Cyc. 7, 811-841.
906 Powell, T.L., Starr, G., Clark, K.L., Martin, T.A., Gholz, H.L., 2005. Ecosystem and
907 understory water and energy exchange for a mature, naturally
908 regenerated pine flatwoods forest in north Florida. Can. J. For. Res. 35, 1568-1580.

909 Rahman, A.F., Sims, D.A., Cordova, V.D., and El-Masri, B.Z., 2005. Potential of MODIS EVI
910 and surface temperature for directly estimating per-pixel ecosystem C fluxes. *Geophy. Res.*
911 *Lett. 32,* L19404, doi:10.1029/2005GL024127.
912 Ranson, K.J., Daughtry, C.S.T., Biehl, L.L., Bauer, M.E., 1985. Sun-view angle effects on
913 reflectance factors of corn canopies. Remote Sens. Environ. 18, 147-161.
914 Reichstein, M., Falge, E., Baldocchi, D., Papale, D., Aubinet, M., Berbigier, P., Bernhofer, C.,
915 Buchmann, N., Gilmanov, T., Granier, A., Grunwald, T., Havrankova, K., Ilvesniemi, H.,
916 Janous, D., Knohl, A., Laurila, T., Lohila, A., Loustau, D., Matteucci, G., Meyers, T.,
917 Miglietta, F., Ourcival, J. M., Pumpanen, J., Rambal, S., Rotenberg, E., Sanz, M.,
918 Tenhunen, J., Seufert, G., Vaccari, F., Vesala, T., Yakir, D., and Valentini, R. (2005), On
919 the separation of net ecosystem exchange into assimilation and ecosystem respiration:
920 review and improved algorithm, *Global Change Biol., 11*, 1424-1439.
921 Richardson, A.D., Hollinger, D.Y., Aber, J.D., Qllinger, S.V., Braswell, B.H., 2007.
922 Environmental variation is directly responsible for short- but not long-term variation in
923 forest-atmosphere carbon exchange. Global Change Biol. 13, 788-803.
924 Richardson, A.D., Mahecha, M.D., Falge, E., Kattge, J., Moffat, A.M., Papale, D., Reichstein,
925 M., Stauch, V.J., Braswell, B.H., Churkina, G., Kruijt, B., Hollinger, D.Y., 2008. Statistical
926 properties of random CO_2 flux measurement uncertainty inferred from model residuals.
927 Agri. For. Meteor. 148, 38-50.
928 Running, S.W., Hunt, E.R., 1993. Generalization of a forest ecosystem process model for other
929 biomes, Biome-BGC, and an application for global-scale models. Scaling processes
930 between leaf and landscape levels. In: *Scaling Physiological Processes: Leaf to Globe*
931 (Ehleringer J. R., Field C. B., eds.), pp. 141-158. Academic Press, San Diego.

Running, S.W., Baldocchi, D.D., Turner, D.P., Gower, S.T., Bakwin, P.S., Hibbard, K.A., 1999. A global terrestrial monitoring network integrating tower fluxes, flask sampling, ecosystem modeling and EOS satellite data. Remote Sens. Environ. 70, 108-127.

Running, S.W., Nemani, R.R., Heinsch, F.A., Zhao, M., Reeves, M., Hashimoto, H., 2004. A continuous satellite-derived measure of global terrestrial primary production. BioScience 54, 547-560.

Ryan, M.G., Law, B.E., 2005. Interpreting, measuring, and modeling soil respiration, Biogeochemistry 73, 3-27.

Salajanu, D., Jacobs, D.M., 2005. Assessing biomass and forest area classifications from MODIS satellite data while incrementing the number of FIA data panels. In: Pecora 16 "Global Priorities in Land Remote Sensing", October 23-27, 2005, Sioux Falls, South Dakota. 10pp.

Schmid, H.P., 1994. Source areas for scalars and scalar fluxes. Bound. –Layer Meteor. 67, 293-318.

Schmid, H.P., 2002. Footprint modeling for vegetation atmospheric exchange studies.: A review and perspective. Agri. For. Meteor., 113, 159-183.

Schmid, H.P., Grimmond, C.S.B., Cropley, F., Offerle, B., Su, H.B., 2000. Measurements of CO_2 and energy fluxes over a mixed hardwood forest in the mid-western United States, Agri. For. Meteor. 103, 357-374.

Schmidt, K.S., Skidmore, A.K., 2003. Spectral discrimination of vegetation types in a coastal wetland. Remote Sens. Environ. 85, 92-108.

Sellers, P.J., Randall, D.A., Betts, A.K., Hall, F.G., Berry, J.A., Collatz, G.J., Denning, A.S., Mooney, H.A., Nobre, C.A., Sato, N., Field, C.B., & Henderson-sellers, A., 1997.

955 Modeling the exchanges of energy, water, and carbon between continents and the
956 atmosphere. Science 275, 502– 509.
957 Shroyer, J.P., Thompson, C., Brown, R., Ohlenbach, P.D., Fjell, D.L., Staggenborg, S.,
958 Duncan, S., Kilgore, G.L., 1996. Kansas crop planting guide. Publication, Vol. L-818 (pp.
959 2). Manhattan, KS: Kansas State University.
960 Sims, D.A., Rahman, A.F., Cordova, V.D., Baldocchi, D.D., Flanagan, L.B., Goldstein, A.H.,
961 Hollinger, D.Y., Misson, L., Monson, R.K., Schmid, H.P., Wofsy, S.C., Xu, L., 2005.
962 Midday values of gross CO_2 flux and light use efficiency during satellite overpasses can be
963 used to directly estimate eight-day mean flux. Agri. For. Meteor. 131, 1-12.
964 Tans, P.P., Fung, I.Y., Takahashi, T., 1990. Observational constraints on the global
965 atmospheric CO_2 budget. Science 247, 1431-1438.
966 Thornton, P.E., Law, B.E., Gholz, H.L., Clark, K.L., Falge, E., Ellsworth, D.S., Goldstein,
967 A.H., Monson, R.K., Hollinger, D., Falk, M., Chen, J., Sparks, J.P., 2002. Modeling and
968 measuring the effects of disturbance history and climate on carbon and water budgets in
969 evergreen needleleaf forests. Agri. For. Meteor. 113, 185-222.
970 Urbanski, S., Barford, C., Wofsy, S., Kucharik, C., Pyle, E., Budney, J., McKain, K.,
971 Fitzjarrald, D., Czikowsky, M., Munger, J.W., 2007. Factors controlling CO_2 exchange on
972 timescales from hourly to decadal at Harvard Forest. J. Geophys. Res. 112, G02020,
973 doi:10.1029/2006JG000293.
974 Verma, S.B., Dobermann, A., Cassman, K.G., Walters, D.T., Knops, J.M., Arkebauer, T.J.,
975 Suyker, A.E., Burba, G.G., Amos, B., Yang, H., Ginting, D., Hubbard, K.G., Gitelson,
976 A.A., Walter-Shea, E.A., 2005. Annual carbon dioxide exchange in irrigated and rainfed
977 maize-based agroecosystems. Agri. For. Meteor. 131, 77-96.

978 Vermote, E.F., Vermeulen, A., 1999. MODIS Algorithm Technical Background Document –
979 Atmospheric Correction Algorithm: Spectral Reflectances (MOD09), Version 4.0.
980 http://modis.gsfc.nasa.gov/data/atbd/atbd_mod08.pdf.
981 Wan, Z., Zhang, Y., Zhang, Q., Li, Z.-L., 2002. Validation of the land-surface temperature
982 products retrieved from Terra Moderate Resolution Imaging Spectroradiometer data.
983 Remote Sens. Environ. 83, 163-180.
984 Waring, R.H., Franklin, J.F., 1979. Evergreen coniferous forests of the Pacific Northwest.
985 Science 204, 1380-1386.
986 Watts, C.J., Scott, R.L., Garatuza-Payan, J., Rodriguez, J.C., Prueger, J., Kustas, W., Douglas,
987 M., 2007. Changes in vegetation condition and surface fluxes during NAME 2004. J. Clim.
988 20, 1810-1820.
989 Wofsy, S.C., Goulden, M.L., Munger, J.W., Fan, S.-M., Bakwin, P.S., Daube, B.C., Bassow,
990 S.L., Bazzaz, F.A., 1993. Net exchange of CO_2 in a mid-latitude forest. Science 260, 1314-
991 1317.
992 Wylie, B.K., Fosnight, E.A., Gilmanov, T.G., Frank, A.B., Morgan, J.A. et al., 2007. Adaptive
993 data-driven models for estimating carbon fluxes in the Northern Great Plains. Remote
994 Sensing of Environment, 106, 399-413.
995 Xiao, J., Moody, A., 2004a. Trends in vegetation activity and their climatic correlates: China
996 1982 to 1998. Int. J. Remote Sens. 25, 5669-5689.
997 Xiao, J., Moody, A., 2004b. Photosynthetic activity of US biomes: responses to the spatial
998 variability and seasonality of precipitation and temperature. Global Change Biol. 10, 437-
999 451.

1000 Xiao, J., Moody, A., 2005. A comparison of methods for estimating fractional green vegetation
1001 cover within a dsert-to-upland transition zone in central New Mexico, USA. Remote Sens.
1002 Environ. 98, 237-250.
1003 Xiao, J., Zhuang, Q., Liang, E., McGuire, A.D., Kicklighter, D.W., Moody, A., Melillo, J.M.,
1004 2008. Droughts and their impacts on carbon cycling of terrestrial ecosystems during the
1005 20th century, *J. Geophys. Res.*, *revised.*
1006 Xiao, X., Zhang, Q., Saleska, S., Hutyra, L., Camargo, P.D. et al., 2005. Satellite-based
1007 modeling of gross primary production in a seasonally moist tropical evergreen forest.
1008 Remote Sens. Environ. 94, 105-122.
1009 Xu, L., Baldocchi, D.D., 2004. Seasonal variation in carbon dioxide exchange over a
1010 Mediterranean annual grassland in California. Agri. For. Meteor. 123, 79-96.
1011 Yamaji, T., Sakai, T., Endo, T., Baruah, P.J., Akiyama, T., Saigusa, N., Nakai, Y., Kitamura,
1012 K., Ishizuka, M., Yasuoka, Y., 2007. Scaling-up technique for net ecosystem productivity
1013 of deciduous broadleaved forests in Japan using MODIS data. Ecol. Res.
1014 doi:10.1007/s11284-007-0438-0.
1015 Yang, L., Huang, C., Homer, C., Wylie, B.K., Coan, M.J., 2003. An approach for mapping
1016 large-area impervious surfaces: synergistic use of Landsat-7 ETM+ and high spatial
1017 resolution imagery. Can. J. Remote Sens. 29, 230-240.
1018 Yang, F., Ichii, K., White, M.A., Hashimoto, H., Michaelis, A.R., Votava, P., Zhu, A.-X.,
1019 Huete, A., Running, S.W., Nemani, R.R., 2007. Developing a continental-scale measure of
1020 gross primary production by combining MODIS and AmeriFlux data through support
1021 machine approach. Remote Sens. Environ. 110, 109-122.

Zhao, M., Heinsch, F.A., Nemani, R.R., Running, S.W., 2005. Improvements of the MODIS terrestrial gross and net primary production global data set. Remote Sens. Environ. 95, 164-175.

Zhuang, Q., McGuire, A.D., O'Neill, K.P., Harden, J.W., Romanovsky, V.E., Yarie, J., 2002. Modeling the soil thermal and carbon dynamics of a fire chronosequence in Interior Alaska, J. Geophy. Res. 107, 8147, doi:10.1029/2001JD001244, 2002.

Zhuang, Q., McGuire, A.D., Melillo, J.M., Clein, J.S., Dargaville, R.J., Kicklighter, D.W., Myneni, R.B., Dong, J., Romanovsky, V.E., Harden, J., Hobbie, J.E., 2003. Carbon cycling in extratropical terrestrial ecosystems of the Northern Hemisphere during the 20th Century: A modeling analysis of the influences of soil thermal dynamics. Tellus 55B, 751-776.

Figure captions:

Fig. 1. Location and spatial distribution of the AmeriFlux sites used in this study. The base map is the reclassified MODIS land-cover map that was used for the continental-scale estimation of NEE. Symbols indicate the location of the AmeriFlux sites.

Fig. 2. Distribution of the 42 AmeriFlux sites in mean annual climate space. Climate parameters are the mean annual precipitation (x-axis) and mean annual temperature (y-axis) taken over a 30-year period of record (1971-2000) from the PRISM database (http://www.prism.oregonstate.edu/). Gray points indicate the climate space distribution of landmass within the conterminous United States. The climate data have been resampled to 12 km resolution for plotting points in this figure. Symbols show the location of each AmeriFlux site in the climate space. The climate data of the sites are from the AmeriFlux website (http://public.ornl.gov/ameriflux/) and the PRISM database.

Fig. 3. Scatterplot of observed 8-day NEE versus predicted 8-day NEE. The solid line is the 1:1 line.

Fig. 4. Scatterplot of predicted 8-day NEE versus residuals (observed - predicted) over the period 2005-2006.

Fig. 5. The average error and relative error averaged across all AmeriFlux sites for each 8-day period.

Fig. 6. Observed and predicted 8-day NEE (g C m^{-2} day^{-1}) for each AmeriFlux site over the period 2005-2006. The green line with square symbols represents the observed values, and the red line with circle symbols represents the predicted values. The x-axis is the Julian day over the period 2005-2006. Site abbreviations are used here, and their full names are given in Table

1. The vegetation type for each site is given in parenthesis: evergreen forests (EF), deciduous forests (DF), mixed forests (MF), shrublands (Sh), savannas (Sa), grasslands (Gr), and croplands (Cr).

Fig. 7. Scatterplot of observed mean NEE versus predicted mean NEE across the AmeriFlux sites. Error bars are standard errors (defined as the standard deviation divided by the square root of the number of observations) of the observed and predicted 8-day mean NEE. Abbreviations of AmeriFlux sites are given in Table 1.

Fig. 8. Scatterplot of observed mean NEE versus predicted mean NEE across vegetation types: EF - evergreen forests; DF - deciduous forests; MF - mixed forests; Sh - shrublands; Sa - savannas; Gr - grasslands; Cr – Croplands. Error bars are standard errors (defined as the standard deviation divided by the square root of the number of observations) of the observed and predicted 8-day mean NEE.

Fig. 9. Examples of estimated 8-day NEE for the conterminous U.S. from January through December in 2005. For each month, the second 8-day NEE composite is shown here. The units are g C m^{-2} day^{-1}. Positive values indicate carbon release, and negative values indicate carbon uptake.

Fig. 10. Predicted NEE for each season in 2005: (a) spring (March-May); (b) summer (June-August); (c) fall (September-November); (d) winter (December-February). The units are g C m^{-2} $season^{-1}$. Positive values indicate carbon release, and negative values indicate carbon uptake.

Fig. 11. Estimated mean and total 8-day NEE for each vegetation type in the conterminous U.S. in 2005. (a) Mean 8-day NEE (g C m^{-2} day^{-1}); (b) Total 8-day NEE (Tg C day^{-1}). Inset in

plot (b) indicates the area (10^6 km^2) of each vegetation type: evergreen forests (EF), deciduous forests (DF), mixed forests (MF), shrublands (Sh), savannas (Sa), grasslands, (Gr), and croplands (Cr). The x axis is labeled with both 8-day composite number and the starting date (month/day) of each composite.

Table 1. Site descriptions including name, latitude, longitude, vegetation structure, years of data available, and references for each flux site in this study.

Site	State	Lat	Lon	Vegetation structure	Vegetation type	Year	References
Audubon Research Ranch (ARR)	AZ	31.59	-110.51	Desert grasslands	Grasslands	2002-2006	
Santa Rita Mesquite (SRM)	AZ	31.82	-110.87	Mesquite-dominated savanna	Savannas	2004-2006	Watts et al., 2007
Walnut Gulch Kendall Grasslands (WGK)	AZ	31.74	-109.94	Warm season C4 grassland	Grasslands	2004-2006	
Sky Oaks Old Stand (SOO)	CA	33.37	-116.62	Chaparral (Mediterranean-type ecosystems)	Shrublands	2004-2006	Lipson et al., 2005
Sky Oaks Young stand (SOY)	CA	33.38	-116.62	Chaparral (Mediterranean-type ecosystems)	Shrublands	2001-2006	Lipson et al., 2005
Tonzi Ranch (TR)	CA	38.43	-120.97	Oak savanna, grazed grassland dominated by blue oak and grasses	Savannas	2001-2006	Ma et al., 2007
Vaira Ranch (VR)	CA	38.41	-120.95	Grazed C3 grassland opening in a region of oak/grass savanna	Grasslands	2001-2006	Xu and Baldocchi, 2004
Niwot Ridge Forest (NRF)	CO	40.03	-105.55	Subalpine coniferous forest dominated by subalpine, Engelmann spruce, and lodgepole pine	Evergreen forests	2000-2003	Monsoon et al., 2002
Kennedy Space Center - Scrub Oak (KSC)	FL	28.61	-80.67	Scrub-oak palmetto dominated by schlerophyllous evergeen oaks and the Saw Palmetto Serenoa repens	Shrublands	2000-2006	Dore et al., 2003
Austin Cary - Slash Pine (AC)	FL	29.74	-82.22	Naturally regenerated pine dominated by Pinus palustris/Pinus ellottii	Evergreen forests	2001-2005	Powell et al., 2005
Bondville (Bon)	IL	40.01	-88.29	Annual rotation between corn (C4) and soybeans (C3)	Croplands	2001-2006	Hollinger et al., 2005
FNAL agricultural site (FAg)	IL	41.86	-88.22	Soybean/corn	Croplands	2005-2006	
FNAL Prairie site (FPr)	IL	41.84	-88.24	Tall grass prairie	Grasslands	2004-2006	
Morgan Monroe State Forest (MMS)	IN	39.32	-86.41	Mixed hardwood deciduous forest dominated by sugar maple, tulip poplar, sassafras, white oak, and black oak	Deciduous forests	2000-2005	Schmid et al., 2000
Harvard Forest EMS Tower (HFE)	MA	42.54	-72.17	Temperate deciduous forest dominated by red oak, red maple, black birch, white pine, and hemlock	Deciduous forests	2000-2004	Urbanski et al. 2007
Harvard Forest Hemlock Site (HFH)	MA	42.54	-72.18	Temperate coniferous forest dominated by hemlock	Evergreen forests	2004	

Little Prospect Hill (LPH)	MA	42.54	-72.18	Temperate deciduous forest dominated by red oak, red maple, black birch, white pine, and hemlock	Deciduous forests	2002-2005	
Howland forest (HF)	ME	45.20	-68.74	Boreal--northern hardwood transitional forest consisting of hemlock-spruce-fir, aspen-birch, and hemlock-hardwood mixtures	Evergreen forests	2000-2004	Hollinger et al., 1999, 2004
Howland forest (west tower) (HFW)	ME	45.21	-68.75	Deciduous needle forest, Boreal/northern hardwood ecoton, old coniferous	Deciduous forests	2000-2004	Hollinger et al., 1999, 2004
Sylvania Wilderness Area (SWA)	MI	46.24	-89.35	Old-growth eastern hemlock/sugar maple/basswood/yellow birch	Mixed forests	2002-2006	Desai et al., 2005
Univ. of Mich. Biological Station (UMB)	MI	45.56	-84.71	Mid-aged conifer and deciduous, northern hardwood, pine understory, aspen, mostly deciduous, old growth hemlock	Mixed forests	2000-2003	Gough et al., 2008
Missouri Ozark (MO)	MO	38.74	-92.20	Oak hickory forest	Deciduous forests	2004-2006	Gu et al. 2006, 2007
Goodwin Creek (GC)	MS	34.25	-89.97	Temperate grassland	Grasslands	2002-2006	
Fort Peck (FPe)	MT	48.31	-105.10	Grassland	Grasslands	2000-2006	
Duke Forest loblolly pine (DFP)	NC	35.98	-79.09	Even-aged loblolly pine forest	Evergreen forests	2001-2005	Oren et al. 1998, 2006
Duke Forest hardwoods (DFH)	NC	35.97	-79.10	An uneven-aged closed-canopy stand in an oak-hickory type forest composed of mixed hardwood species with pine (P. taeda) as a minor component	Deciduous forests	2003-2005	Pataki and Oren, 2003
North Carolina loblolly pine (NCP)	NC	35.80	-76.67	Loblolly pine plantation	Evergreen forests	2005-2006	
Mead -irrigated continuous maize site (MIC)	NE	41.17	-96.48	Continuous maize	Croplands	2001-2005	Verma et al. 2005
Mead irrigated rotation (MIR)	NE	41.16	-96.47	Maize-soybean rotation	Croplands	2001-2005	Verma et al. 2005
Mead rainfed (MR)	NE	41.18	-96.44	Maize-soybean rotation	Croplands	2001-2005	Verma et al. 2005
Bartlett Experimental Forest (BEF)	NH	44.06	-71.29	Temperate northern hardwood forest dominated by American beech, red maple, paper birch, and hemlock	Deciduous forests	2004-2005	Jenkins et al., 2007
Toledo Oak Openings (TOP)	OH	41.55	-83.84	Oak Savannah dominated by quercus rebrua, quercus alba, and acer rubrum	Savannas	2004-2005	
ARM Oklahoma (ARM)	OK	36.61	-97.49	Winter wheat, some pasture and summer crops	Croplands	2003-2006	
Metolius intermediate aged ponderosa pine (MI)	OR	44.45	-121.56	Temperate coniferous forest dominated by pinus ponderosa, purshia tridentate, arctostaphylos patula	Evergreen forests	2003-2005	Law et al. 2003; Irvine et al. 2007
Metolius new young pine	OR	44.32	-121.61	Temperate coniferous forest dominated by pinus	Evergreen forests	2004-2005	Law et al.

(MN)				ponderosa and purshia tridentata			2003; Irvine et al. 2007
Brookings (Bro)	SD	44.35	-96.84	Temperate grassland	Grasslands	2004-2006	
Freeman Ranch Mesquite Juniper (FRM)	TX	29.95	-98.00	Grassland in transition to an Ashe juniper-dominated woodland	Savannas	2004-2006	
Wind River Crane Site (WRC)	WA	45.82	-121.95	Temperate coniferous forest dominated by douglas-fir and western hemlock	Evergreen forests	2000-2004	Falk et al., 2008
Lost Creek (LC)	WI	46.08	-89.98	Alder-willow deciduous wetland	Deciduous forests	2000-2005	
Willow Creek (WC)	WI	45.81	-90.08	Temperate/Boreal forest dominated by white ash, sugar maple, basswood, green ask, and red oak	Deciduous forests	2000-2006	Cook et al., 2004
Wisconsin intermediate hardwood (WIH)	WI	46.73	-91.23		Deciduous forests	2003	
Wisconsin mature red pine (MRP)	WI	46.74	-91.17		Evergreen forests	2002-2005	

Descriptions on vegetation structures are from the site information available at http://public.ornl.gov/ameriflux/ for all sites except Duke Forest - hardwoods. The description on the vegetation for Duke Forest - hardwoods is from http://www.env.duke.edu/other/AMERIFLUX/hwsite.html.

Table 2. The seven broader vegetation types used in the study and the corresponding UMD vegetation classes.

Vegetation types	UMD classes	Definition (Belward and Loveland, 1996)
Evergreen forests	Evergreen needleleaf forests (1), evergreen broadleaf forests (2)	Tree canopy cover > 60% and tree height > 2m. Most of the canopy remains green all year
Deciduous forests	Deciduous needleleaf forests (3), deciduous broadleaf forests (4)	Tree canopy cover > 60% and tree height > 2m. Most of the canopy is deciduous
Mixed forests	Mixed forests (5)	Tree canopy cover > 60% and tree height > 2m. Mixed evergreen and deciduous canopy
Shrublands	Closed shrublands (6), open shrublands (7)	Shrub canopy cover > 10% (10-60% for open shrublands, >60% for closed shrublands) and height < 2m
Savannas	Woody savannas (8), savannas (9)	Forest canopy cover between 10-60% (30-60% for woody savannas, 10-30% for savannas) and height > 2m
Grasslands	Grasslands (10)	Herbaceous cover. Woody cover < 10%
Croplands	Croplands (12)	Temporary crops followed by harvest and a bare soil period

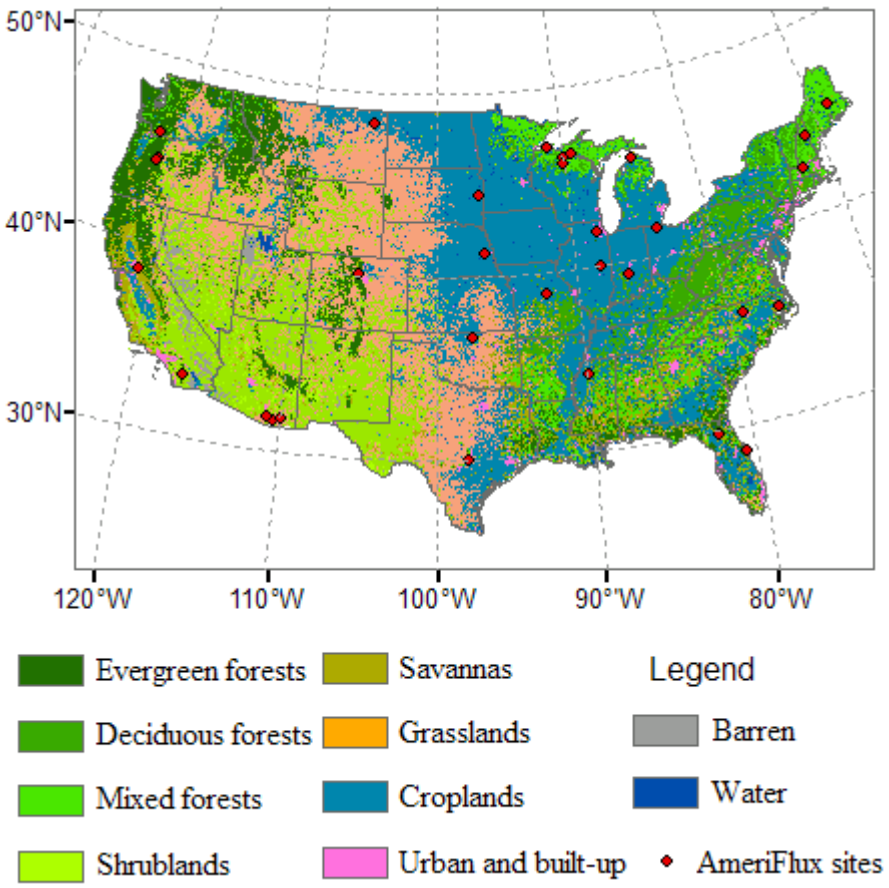
50°N
40°N
30°N
120°W
110°W
100°W
90°W
80°W
Legend
Evergreen forests
Deciduous forests
Mixed forests
Shrublands
Savannas
Grasslands
Croplands
Urban and built-up
Barren
Water
AmeriFlux sites

Fig. 1.

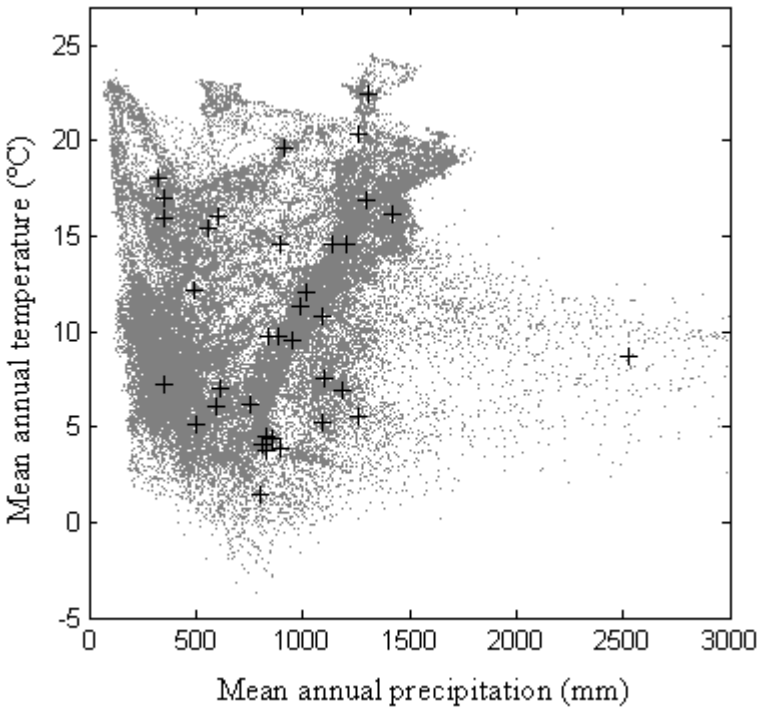
Mean annual temperature (°C)
25
20
15
10
5
0
-5
0
500
1000
1500
2000
2500
3000
Mean annual precipitation (mm)

Fig. 2.

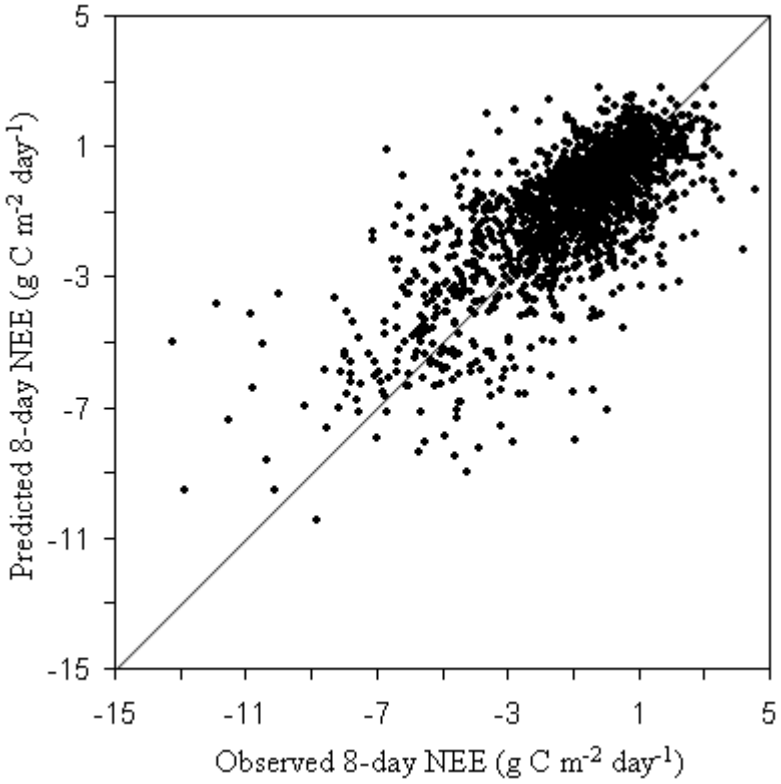
5
1
-3
-7
-11
-15
-15
-11
-7
-3
1
5
Predicted 8-day NEE (g C m-2 day-1)
Observed 8-day NEE (g C m-2 day-1)

Fig. 3.

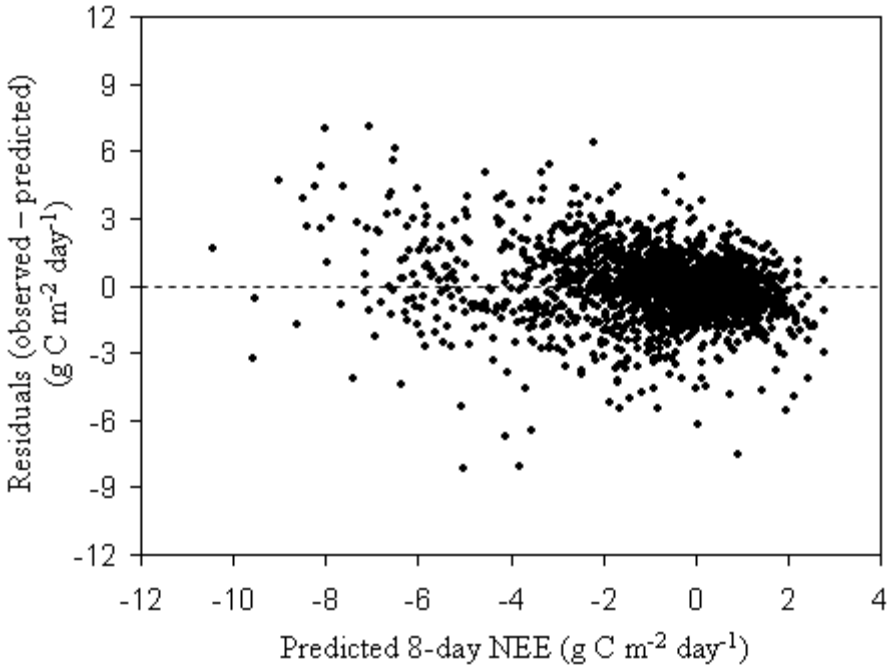
Residuals (observed – predicted)
(g C m-2 day-1)
12
9
6
3
0
-3
-6
-9
-12
-12
-10
-8
-6
-4
-2
0
2
4
Predicted 8-day NEE (g C m-2 day-1)

Fig. 4.

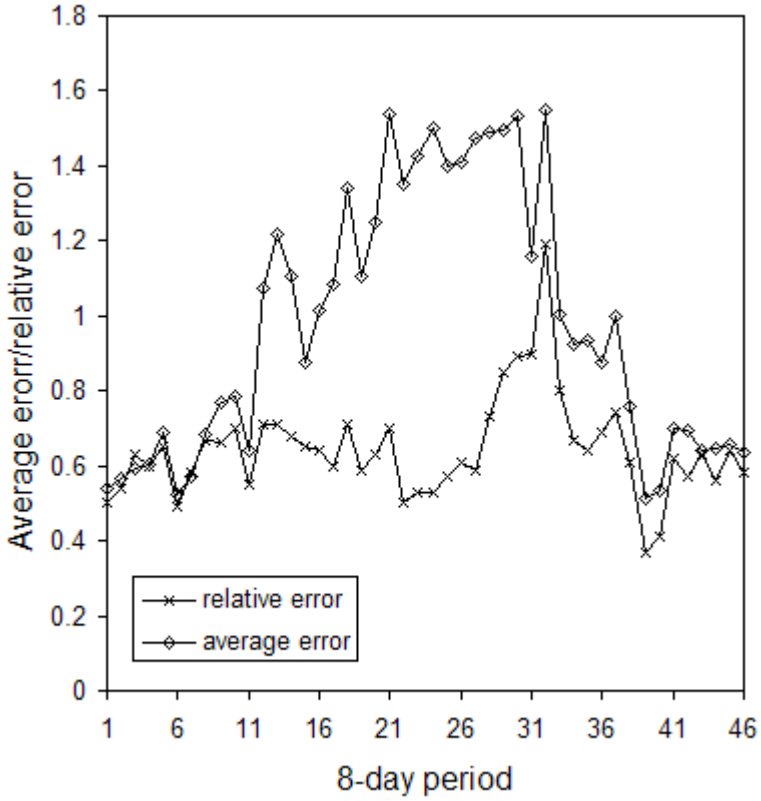
Average erorr/relative error
8-day period
relative error
average error
0
0.2
0.4
0.6
0.8
1
1.2
1.4
1.6
1.8
1
6
11
16
21
26
31
36
41
46

Fig. 5.

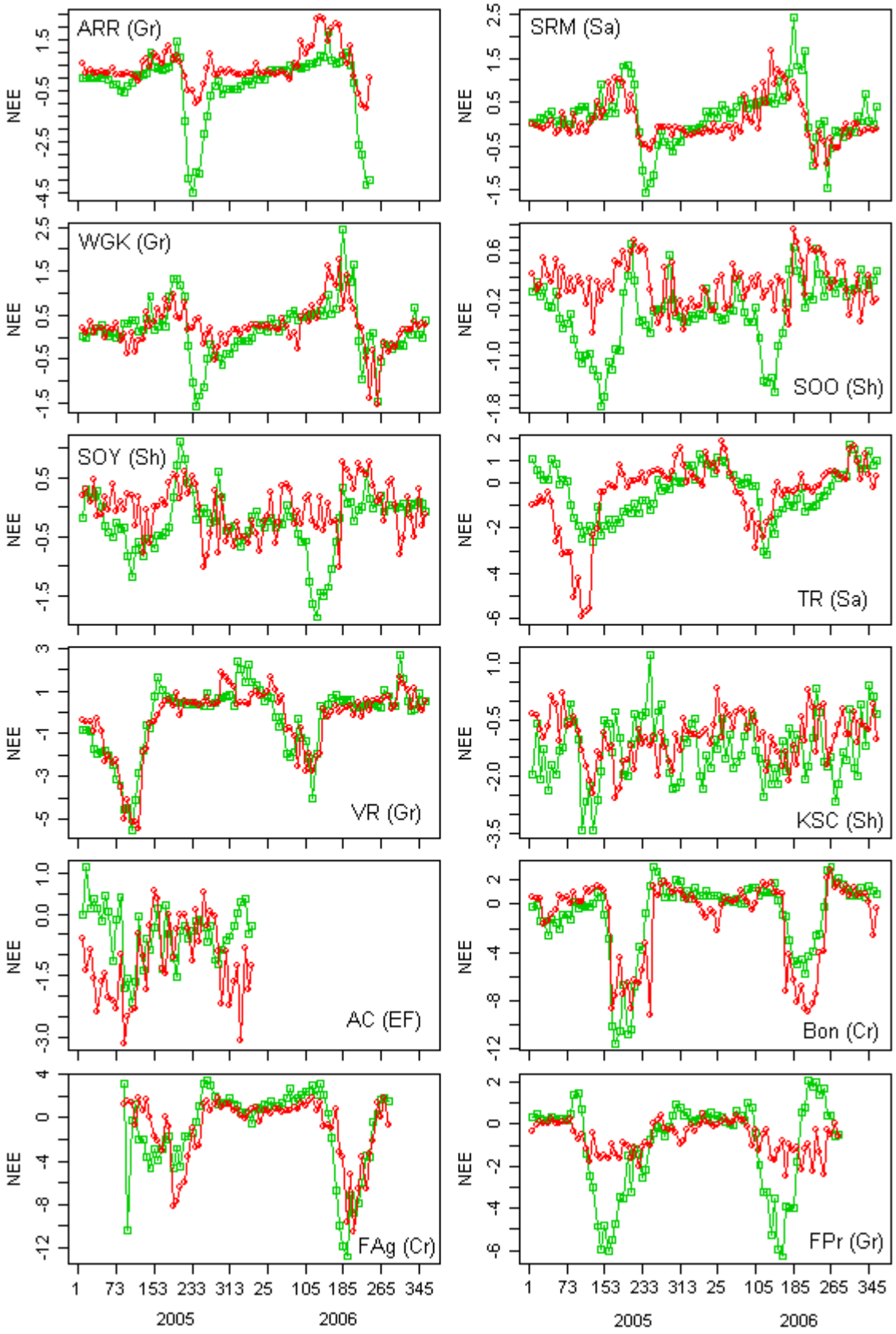
ARR (Gr)
SRM (Sa)
WGK (Gr)
SOO (Sh)
SOY (Sh)
TR (Sa)
VR (Gr)
KSC (Sh)
AC (EF)
Bon (Cr)
FAg (Cr)
FPr (Gr)
NEE
1 73 153 233 313 25 105 185 265 345
2005
2006

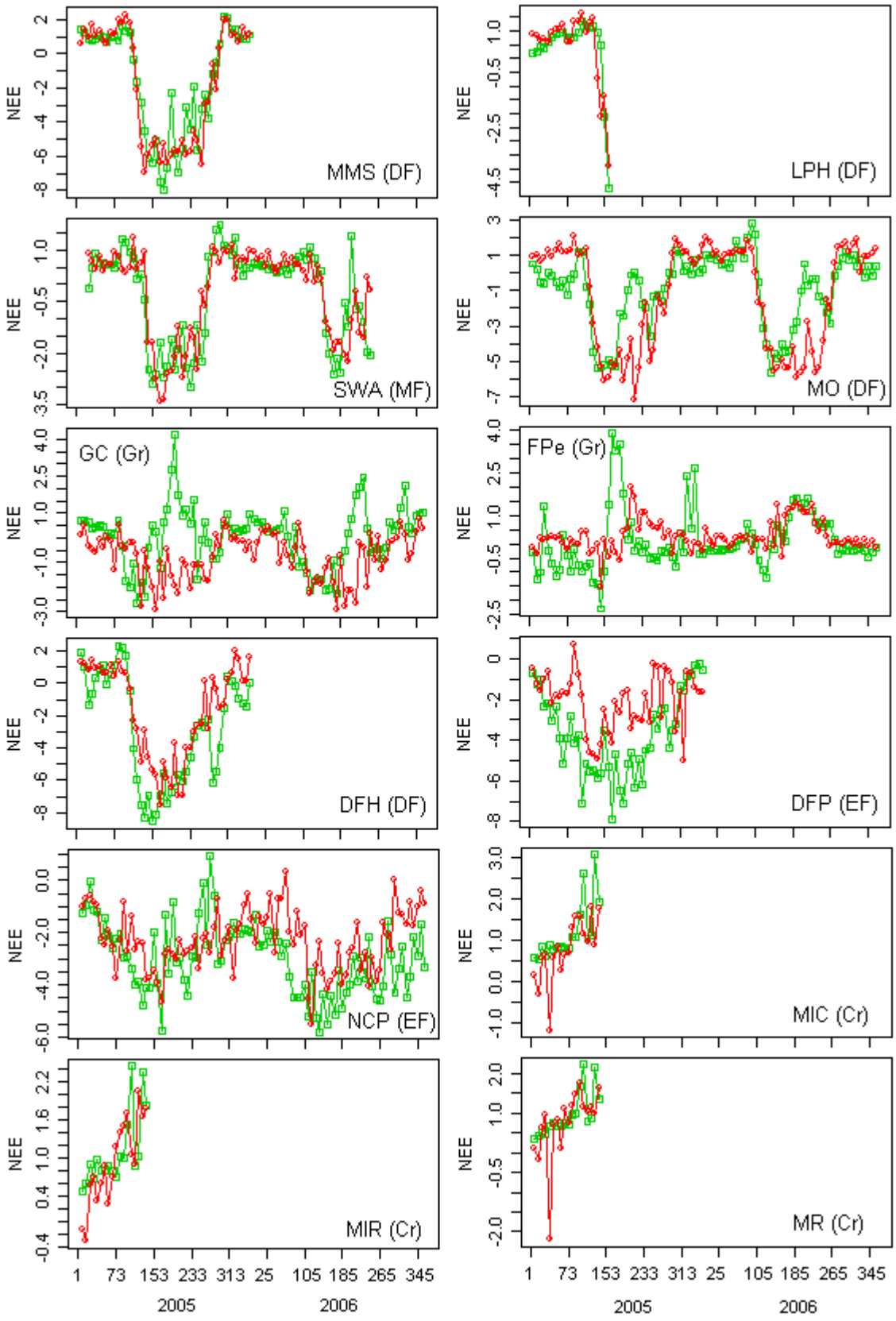
MMS (DF)
LPH (DF)
SWA (MF)
MO (DF)
GC (Gr)
FPe (Gr)
DFH (DF)
DFP (EF)
NCP (EF)
MIC (Cr)
MIR (Cr)
MR (Cr)
NEE
1 73 153 233 313 25 105 185 265 345
2005
2006

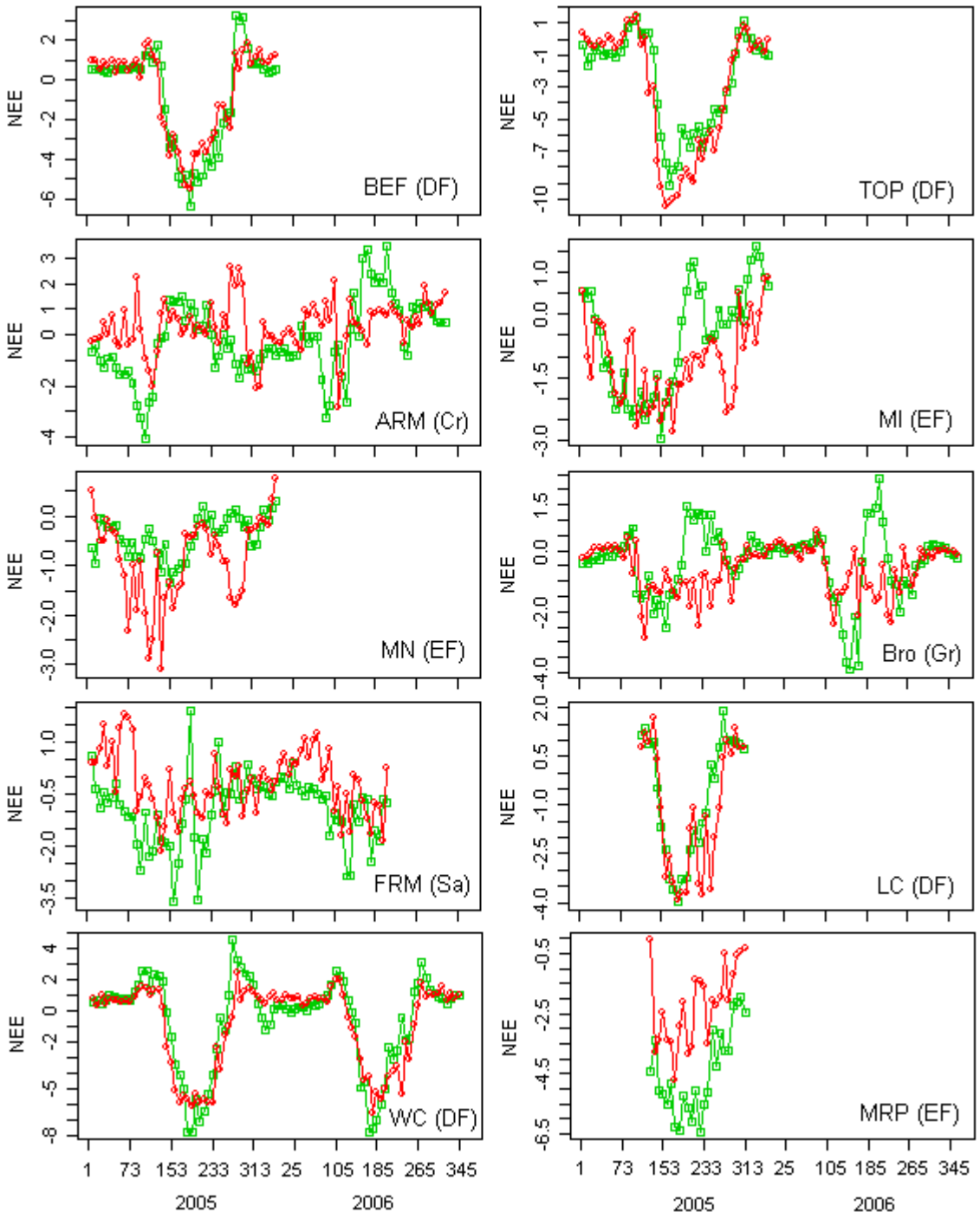
NEE
BEF (DF)
TOP (DF)
ARM (Cr)
MI (EF)
MN (EF)
Bro (Gr)
FRM (Sa)
LC (DF)
WC (DF)
MRP (EF)
1 73 153 233 313 25 105 185 265 345
2005
2006

Fig. 6.

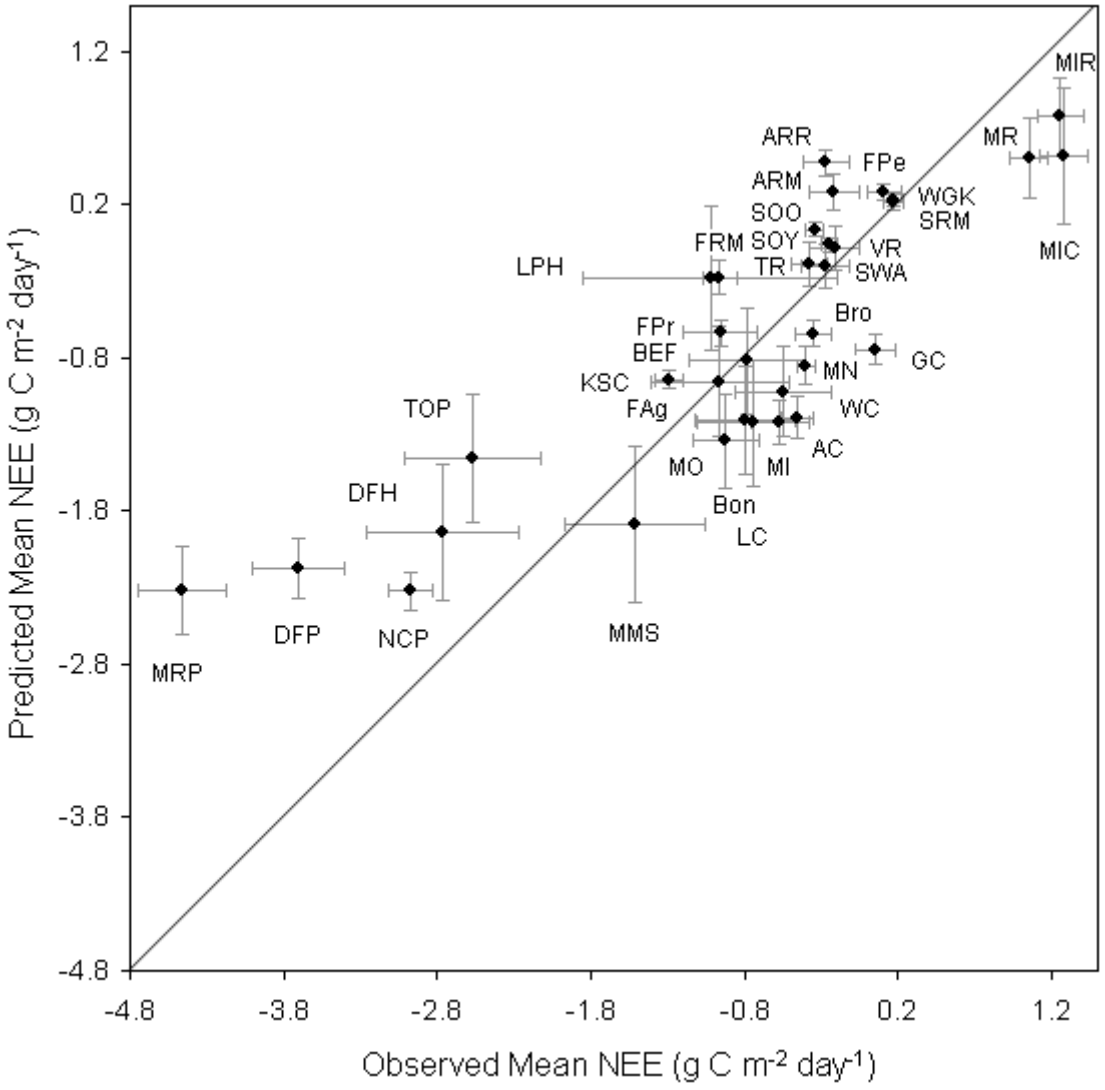
Predicted Mean NEE (g C m-2 day-1)
Observed Mean NEE (g C m-2 day-1)
1.2
0.2
-0.8
-1.8
-2.8
-3.8
-4.8
-4.8
-3.8
-2.8
-1.8
-0.8
0.2
1.2
MIR
MR
MIC
ARR
FPe
ARM
WGK
SRM
SOO
SOY
FRM
VR
TR
SWA
LPH
Bro
FPr
BEF
GC
MN
KSC
FAg
WC
AC
MO
MI
Bon
LC
TOP
DFH
MRP
DFP
NCP
MMS

Fig. 7.

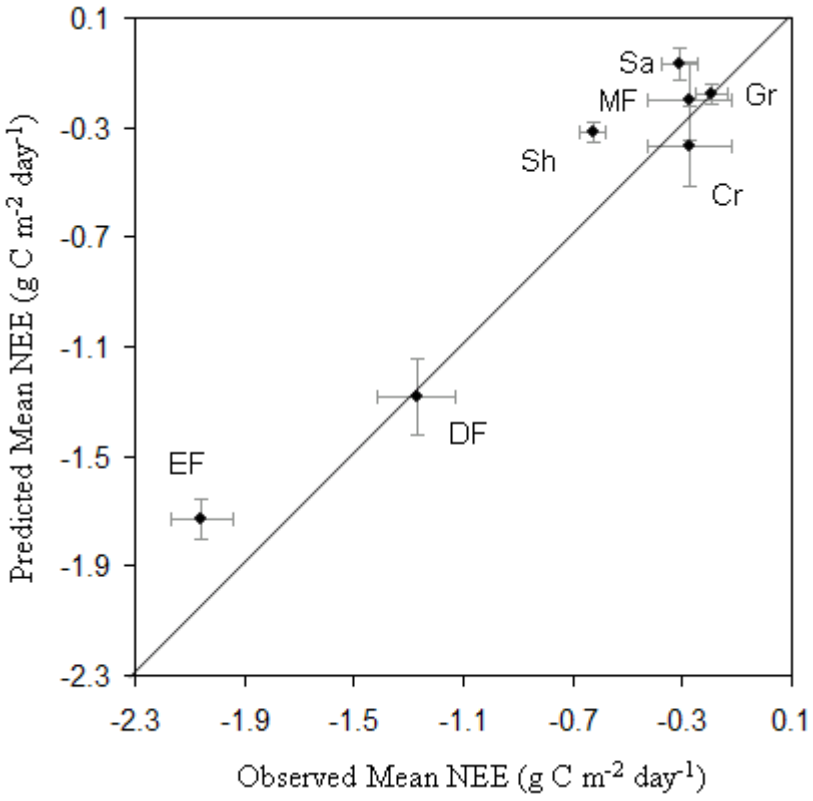
0.1
-0.3
-0.7
-1.1
-1.5
-1.9
-2.3
Predicted Mean NEE (g C m-2 day-1)
-2.3
-1.9
-1.5
-1.1
-0.7
-0.3
0.1
Observed Mean NEE (g C m-2 day-1)
Sa
MF
Gr
Sh
Cr
DF
EF

Fig. 8.

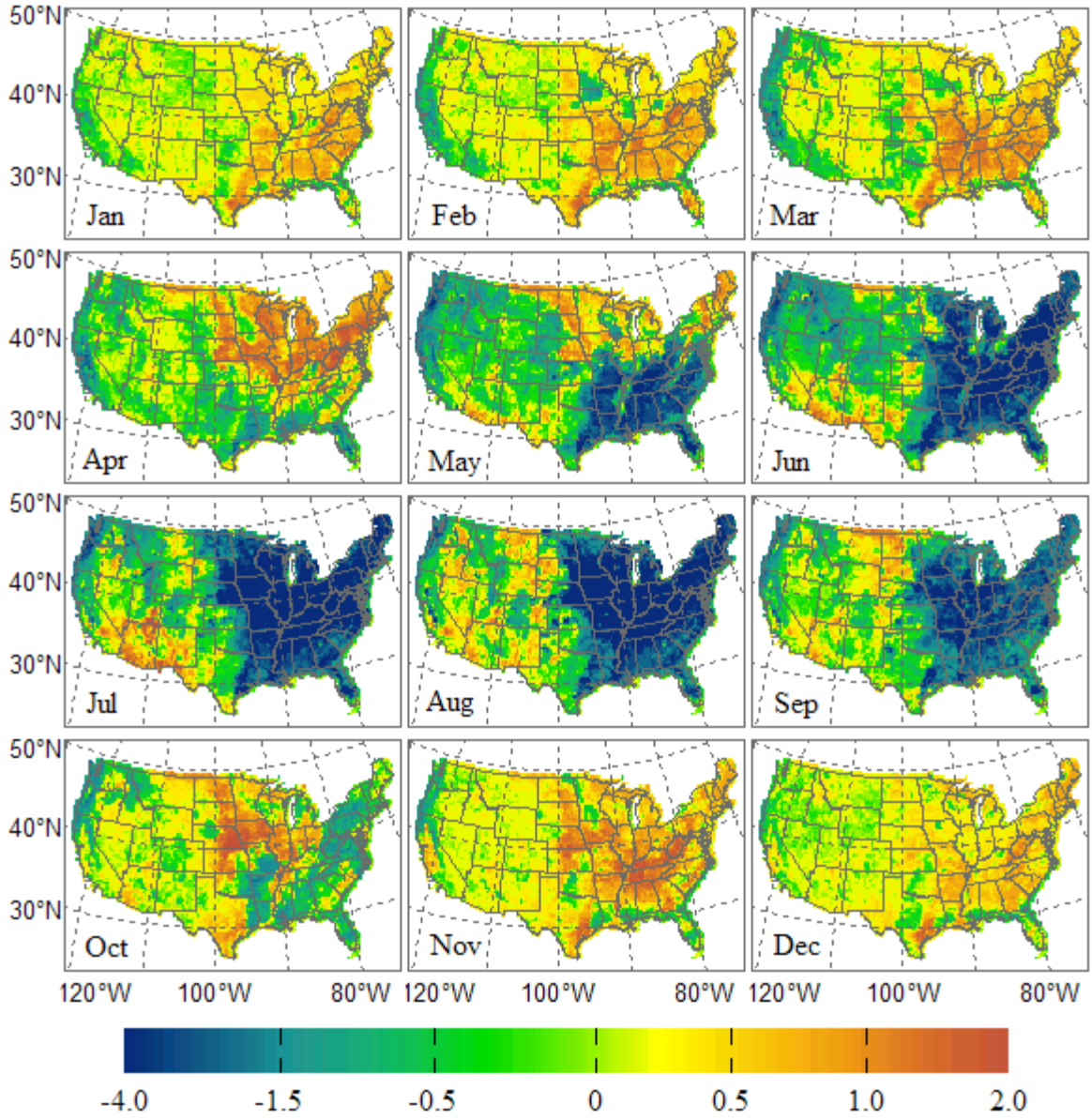
50°N
40°N
30°N
Jan
Feb
Mar
Apr
May
Jun
Jul
Aug
Sep
Oct
Nov
Dec
120°W
100°W
80°W
-4.0
-1.5
-0.5
0
0.5
1.0
2.0

Fig. 9.

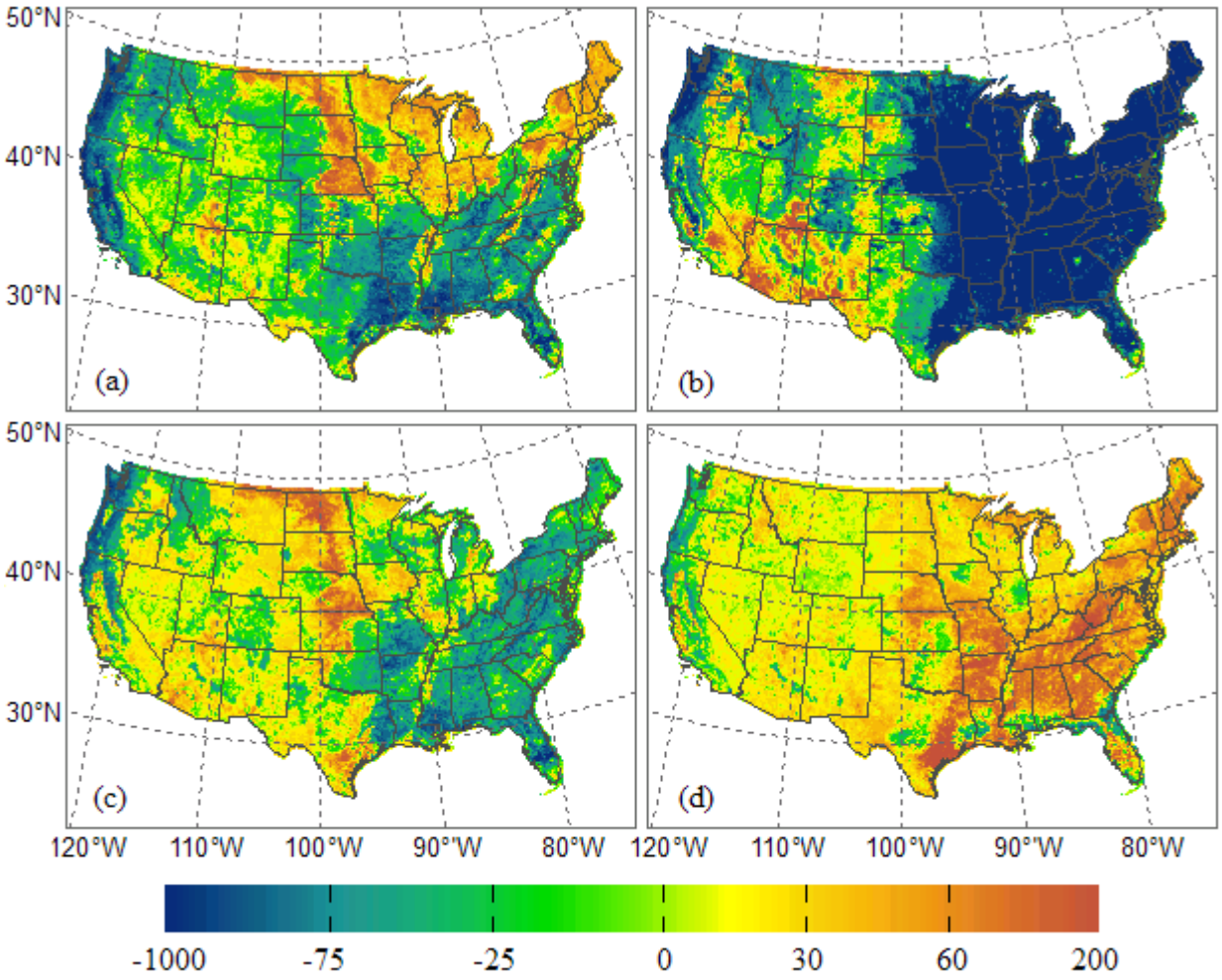

Fig. 10.

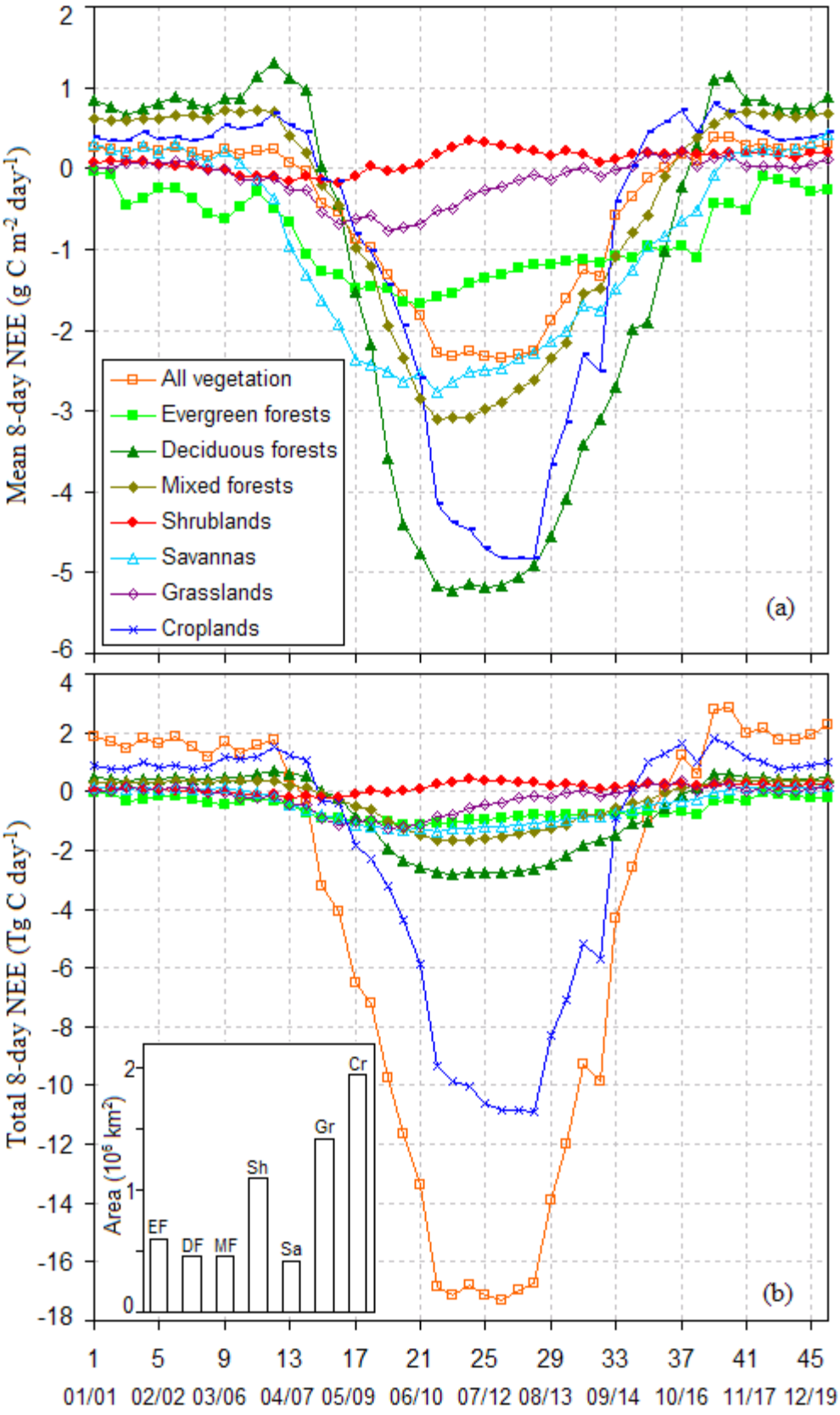
Mean 8-day NEE (g C m-2 day-1)
All vegetation
Evergreen forests
Deciduous forests
Mixed forests
Shrublands
Savannas
Grasslands
Croplands
(a)
Total 8-day NEE (Tg C day-1)
Area (10^6 km^2)
EF
DF
MF
Sh
Sa
Gr
Cr
(b)
1 5 9 13 17 21 25 29 33 37 41 45
01/01 02/02 03/06 04/07 05/09 06/10 07/12 08/13 09/14 10/16 11/17 12/19

Fig. 11.